© 2014. Published by The Company of Biologists Ltd | Journal of Cell Science (2014) 127, 1660–1671 doi:10.1242/jcs.131284

RESEARCH ARTICLE

Adhesive interactions of N-cadherin limit the recruitment of microtubules to cell–cell contacts through organization of actomyosin

Charlotte Plestant[1], Pierre-Olivier Strale[1], Rima Seddiki[1,2], Emmanuelle Nguyen[3], Benoit Ladoux[2,3] and René-Marc Mège[1,*]

ABSTRACT

Adhesive interactions of cadherins induce crosstalk between adhesion complexes and the actin cytoskeleton, allowing strengthening of adhesions and cytoskeletal organization. The underlying mechanisms are not completely understood, and microtubules (MTs) might be involved, as for integrin-mediated cell–extracellular-matrix adhesions. Therefore, we investigated the relationship between N-cadherin and MTs by analyzing the influence of N-cadherin engagement on MT distribution and dynamics. MTs progressed less, with a lower elongation rate, towards cadherin adhesions than towards focal adhesions. Increased actin treadmilling and the presence of an actomyosin contractile belt, suggested that actin relays inhibitory signals from cadherin adhesions to MTs. The reduced rate of MT elongation, associated with reduced recruitment of end-binding (EB) proteins to plus ends, was alleviated by expression of truncated N-cadherin, but was only moderately affected when actomyosin was disrupted. By contrast, destabilizing actomyosin fibers allowed MTs to enter the adhesion area, suggesting that tangential actin bundles impede MT growth independently of MT dynamics. Blocking MT penetration into the adhesion area strengthened cadherin adhesions. Taken together, these results establish a crosstalk between N-cadherin, F-actin and MTs. The opposing effects of cadherin and integrin engagement on actin organization and MT distribution might induce bias of the MT network during cell polarization.

KEY WORDS: Actin cytoskeleton, Actin treadmilling, Adherens junctions, Actomyosin, Microtubule dynamics, Cell polarization

INTRODUCTION

During normal development and in pathological contexts (such as cancer), opportunistic cell–cell contacts either are self-reinforcing, leading to the formation of stable intercellular junctions, or induce cell-contact instability, leading to cell–cell intercalation or even cell migration. Despite their importance, the mechanisms leading to these opposite cell responses are only partially understood. They involve the coordination of complex processes, such as adhesion of the cell membrane to adjacent cells, anchoring of the cytoskeleton to the plasma membrane, cytoskeletal remodeling, regulation of the local stability of membrane and intracellular trafficking. Well-known effectors of these processes are cadherins, catenins and actin, which are part of the multi-molecular complex that links the cytoskeleton, the plasma membrane and the surrounding environment. Another element might be the microtubule (MT) network. Indeed, MTs have been reported to be targeted to and captured at cell–extracellular-matrix focal adhesions (Kaverina et al., 1998). MTs have been implicated in signaling, relaxation and trafficking at integrin-mediated adhesions, leading to destabilization of focal adhesions and an increased rate of turnover, a process that is essential for cell polarization and migration (Huda et al., 2012; Kaverina et al., 1998; Small and Kaverina, 2003; Stehbens and Wittmann, 2012). However, the relationship between cadherins and MTs is still unclear and controversial.

Cadherins are homophilic intercellular adhesion receptors that bind intracellular partners, such as α-catenin and β-catenin, allowing the dynamic anchoring of the adhesion complex to the actin cytoskeleton (Giannone et al., 2009; Mège et al., 2006). E-cadherin induces the formation of stable intercellular adherens-type junctions in epithelial cells (Gumbiner et al., 1988; Mège et al., 1988). However, another cadherin, N-cadherin, which is mostly expressed in neural, endothelial, cardiac and skeletal muscle cells, triggers a wider range of cell responses. Indeed, N-cadherin is responsible for the formation of intercalated disks in the heart (Radice et al., 1997) and apical adherens junctions in neuroepithelial cells (Kadowaki et al., 2007). This molecule sustains the migration of embryonic neuronal precursors (Franco et al., 2011; Jossin and Cooper, 2011), as well as neurite elongation in differentiating neurons (Bard et al., 2008; Boscher and Mège, 2008). The molecular and cellular mechanisms leading to this variety of cell responses are not currently known, but they might involve differential recycling (Kawauchi et al., 2010), anchoring of cadherins to actin networks (Giannone et al., 2009), co-activation of growth factor receptors (Hazan et al., 2004) or other signaling pathways (Ratheesh et al., 2012) that regulate the stability of adhesion complexes, organization of the cytoskeleton and cell polarity.

The MT network, which might participate in functional interactions with both cadherins and actin (Stehbens et al., 2009), is an important effector of this cellular plasticity. MTs extend from the centrosome into the cytoplasmic space by growth at their highly dynamic plus end. In so doing, they participate in the maintenance of cell shape and allow the intracellular transport of vesicles by their association with motor proteins. These

[1]Institut du Fer à Moulin, UMRS 839 INSERM, Université Pierre et Marie Curie, 75005 Paris, France. [2]Institut Jacques Monod, UMR7592 CNRS, Université Paris Diderot, 75013 Paris, France. [3]Mechanobiology Institute, National University of Singapore, 117411 Singapore.

*Author for correspondence (mege.rene-marc@ijm.univ-paris-diderot.fr)

Received 2 April 2013; Accepted 18 January 2014

Journal of Cell Science

Journal of Cell Science (2014) 127, 1660–1671 doi:10.1242/jcs.131284

centrosomal MTs are oriented towards the cell cortex and, in particular, towards cadherin-mediated contacts (Shaw et al., 2007; Stehbens et al., 2006). The plus ends of MTs could be at least transiently anchored to adhesion areas through dynein (Ligon and Holzbaur, 2007; Ligon et al., 2001) and MT plus-end tracking proteins, such as CLIP-170 (Stehbens et al., 2006), $p150^{Glued}$ (also known as DCTN1) (Shaw et al., 2007) or IQGAP1 (Fukata et al., 2002; Watanabe et al., 2009). These MTs would then mediate the delivery of cadherin-containing vesicles to the plasma membrane (Chen et al., 2003; Mary et al., 2002; Teng et al., 2005), or the delivery of other junctional proteins (Shaw et al., 2007). Unusually, in polarized epithelial cells, some MTs are directed by their minus ends to the apical junctional complexes (Bacallao et al., 1989), where they have been reported to anchor to adherens junctions (Meng et al., 2008). E-cadherin-mediated adhesion has been reported to influence the dynamics of these noncentrosomal MTs by stabilizing their minus ends (Chausovsky et al., 2000; Shtutman et al., 2008). Most of these studies report on the relationship between cadherins and MTs during adhesion strengthening and epithelial cell polarization, although the crosstalk between cadherin-mediated adhesion and MTs might also be involved in so-called front–rear polarization. Indeed, different MT capture or different regulation of MT dynamics by cell–cell adhesions and focal adhesion complexes might be central to the polarization of cells emigrating from epithelial sheets *in vivo* or from the edge of a wound *in vitro*. In support of this hypothesis, many studies report on the polarization of the MT network and the associated organelles – the centrosome, nucleus and Golgi – at early stages of cell migration *in vitro* (Desai et al., 2009; Dupin et al., 2009; Gomes et al., 2005; Nabi, 1999).

Therefore, we studied and compared the influence of N-cadherin-mediated and integrin-mediated adhesion on MT recruitment and dynamics in the context of their controlled adhesive interactions. To do this, we used surfaces coated with recombinant Ncad–Fc (the cadherin extracellular domain fused to the immunoglobulin Fc fragment) or fibronectin (FN) to investigate the effects of N-cadherin- and integrin-mediated adhesion, respectively (Lambert et al., 2000). MT distribution and dynamics were analyzed by using imaging of fixed and live cells, revealing an inhibitory effect of N-cadherin engagement on both the dynamics of MTs and the targeting of their plus ends towards cadherin adhesions. The reduction in MT plus-end dynamics was specific to N-cadherin engagement, but could not explain the fact that MTs avoid the zones where cadherin adhesions are formed in the lamellipodium. We discovered that N-cadherin engagement sustains a fast actin retrograde flow and the stabilization of an actomyosin belt at the rear of this adhesion zone. Pharmacological perturbations indicated that this contractile tangential arc of actomyosin was the main obstacle to the growth of MT plus ends into the adhesion zone. The opposing effects of cadherin and integrin engagement on actin organization and MT recruitment was confirmed on substrates made of alternating stripes of Ncad–Fc and FN, which eliminated cell shape and global cell-polarization signaling issues. Finally, pharmacological perturbations also suggested that MTs invading the adhesion areas might destabilize N-cadherin-associated adhesion complexes in these cells. Taken together, these results establish the existence of a functional crosstalk between N-cadherin adhesion, F-actin and MT organization. They reveal that cadherin adhesions and focal adhesions mediate different organization of actomyosin and different regulation of the recruitment and dynamics of MTs. These differences might be instrumental in establishing the spatial positioning of organelles and motility machinery that characterizes the polarization of migrating cells.

RESULTS

MTs are directed towards N-cadherin-mediated cell–cell contacts but are maintained at a distance from them

As reported in other cell types (Stehbens et al., 2006; Waterman-Storer et al., 2000), we observed that MTs are directed towards cell–cell contacts formed between murine myoblast C2C12 cells (Fig. 1A). Although it was very difficult to determine whether MTs in the vicinity of β-catenin-labeled areas are associated with the cell membrane or with the cell–substratum interface underneath, it seemed that MTs did not reach β-catenin-labeled cell–cell contacts even though they extended up to the contact-free edges of the cells. This observation was further supported by an analysis of MT distribution in cell doublets spread on FN-coated micropatterns. The micropatterns were designed to impose a specific shape and orientation on cadherin-mediated contacts and to spatially segregate cadherin-mediated contacts from integrin-mediated cell–substratum contacts (Fig. 1B). Under these conditions, some MTs were directed towards cell–cell contacts; however, their recruitment was strongly biased towards cell–substratum contacts, suggesting that cadherin-mediated adhesions might have a repulsive effect on MTs or at least might be less potent than FN adhesions for the recruitment of MTs.

In order to study the specific influence of N-cadherin on MT recruitment, we analyzed the effect of N-cadherin engagement on MT distribution in cells spread on Ncad–Fc substrates, and compared it with the effect of integrin engagement induced by spreading cells on FN (Fig. 1C). On Ncad–Fc, cells extend a large circular lamellipodium that contains radial β-catenin-positive adhesion plaques (cadherin adhesions), mimicking actual mature cell–cell contacts (Gavard et al., 2004). MTs failed to extend far into the region containing N-cadherin adhesions. The few MTs that extended more deeply in the lamellipodium did not colocalize or align with β-catenin-positive adhesion plaques, in contrast to what can be observed in cells spread on FN, in which MTs penetrate up to the edge of the lamellipodium (Fig. 1C). This was confirmed by quantifying the proportion of the whole cell surface that was occupied by the MTs, which was ∼60% for cells spread on Ncad–Fc and 75% for cells spread on FN (Fig. 1D). Quantifying the proportion of the lamellipodial surface (in which the adhesion plaques were concentrated) that was occupied by the MT network revealed an even more striking difference (Fig. 1E), indicating that MTs extend significantly less towards cadherin adhesions than towards focal adhesions. This behavior was not specific to either myogenic cells or N-cadherin, and it could be a more general feature of the consequences of cadherin engagement because a similar failure of MTs to penetrate into adhesive lamellipodia was observed in epithelial Madin-Darby canine kidney (MDCK) cells spread on an E-cadherin–Fc-coated substratum (supplementary material Fig. S1).

In order to prove directly that MT distribution was affected differently by N-cadherin and integrin mobilization within the same cell, C2C12 cells were spread for 2 hours on micropatterned surfaces made of alternating stripes of FN and Ncad–Fc (Fig. 2). Immunofluorescent staining of β-catenin and F-actin revealed that cells formed distinct and specific adhesions on Ncad–Fc versus FN stripes (Fig. 2A,A′). Moreover, cells extended their lamellipodia

Journal of Cell Science (2014) 127, 1660–1671 doi:10.1242/jcs.131284

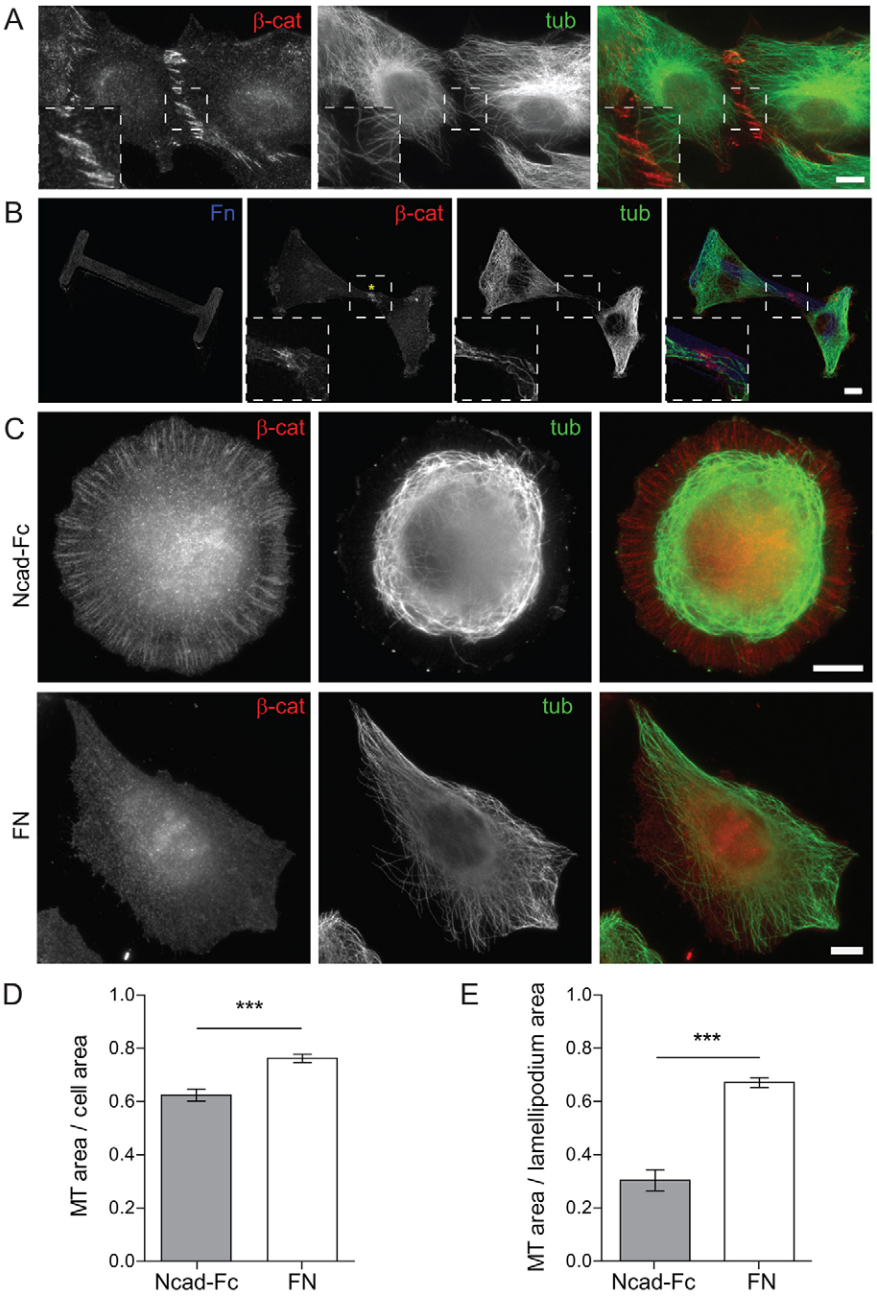

Fig. 1. MTs are directed towards cell–cell contacts but are maintained at a distance by cadherin adhesions. Myogenic C2C12 cells were grown overnight under standard conditions (A) or for 2 h on fibronectin (FN)-coated micropatterns (B), then were fixed and immunostained for β-catenin (β-cat) and α-tubulin (tub). MTs (green) were recruited both at naturally occurring and oriented cell–cell contacts on patterned FN substrates (shown by β-catenin labeling, red). The asterisk (*) shows β-catenin accumulation at the cell–cell contact site. Higher magnifications of the areas delimited by white dotted squares in A and B are represented in the insets. (C) Cells were plated for 2 h on Ncad–Fc or FN substrates. Only a few MTs penetrated the cadherin adhesion areas of cells spread on Ncad–Fc, whereas MTs occupy the whole periphery of cells spread on FN. Scale bars: 10 μm. (D) The fraction of the whole cell surface and (E) of the lamellipodial extensions occupied by the MT network. The data show the means±s.e.m. from three independent experiments, with 10 cells analyzed per condition and per experiment. ***$P<0.0001$ (unpaired Student's *t*-test).

much further on FN than on Ncad–Fc, and they presented very different actin network organization on the two substrates. MTs extended further into the cell extensions formed on FN than those formed on Ncad–Fc substrates (Fig. 2B,B′). To quantify this effect, we determined a penetration index for the MTs, which is the normalized distance of penetration of an individual MT towards the cell edge. The mean MT penetration distance was 0.89±0.01 of the cell radius on FN stripes and 0.78±0.01 of the cell radius on Ncad–Fc stripes (±s.e.m.). These data show that N-cadherin and integrin engagements had specific and distinct effects on both actin and the organization of the MT network.

MT growth is negatively regulated by cadherin engagement

The negative effect of N-cadherin engagement on MTs might be due to a difference in the growth dynamics and stabilization rates of MTs compared with that of integrin engagement. To address this issue, we performed immunolabeling with antibodies against tyrosinated, detyrosinated and acetylated forms of α-tubulin (supplementary material Fig. S2). After 2 hours of spreading on either FN or Ncad–Fc, the MT network predominantly contained tyrosinated α-tubulin and did not contain significant levels of detyrosinated α-tubulin, a result that indicates the presence of unstable recently formed MTs, as expected for cells recovering from the rounding-up induced by passaging (Palazzo et al., 2004). However, cells spread on FN showed the presence of short MT segments that stained for acetylated α-tubulin, whereas no trace of acetylated α-tubulin staining was detected in cells spread on Ncad–Fc, indicating that several stable MTs had formed in this short period on FN, whereas this was not the case on Ncad–Fc. Taken together, these observations indicate that N-cadherin adhesions, in contrast to focal adhesions, might be devoid of signals that attract and/or stabilize MTs or, alternatively, that they

Journal of Cell Science (2014) 127, 1660–1671 doi:10.1242/jcs.131284

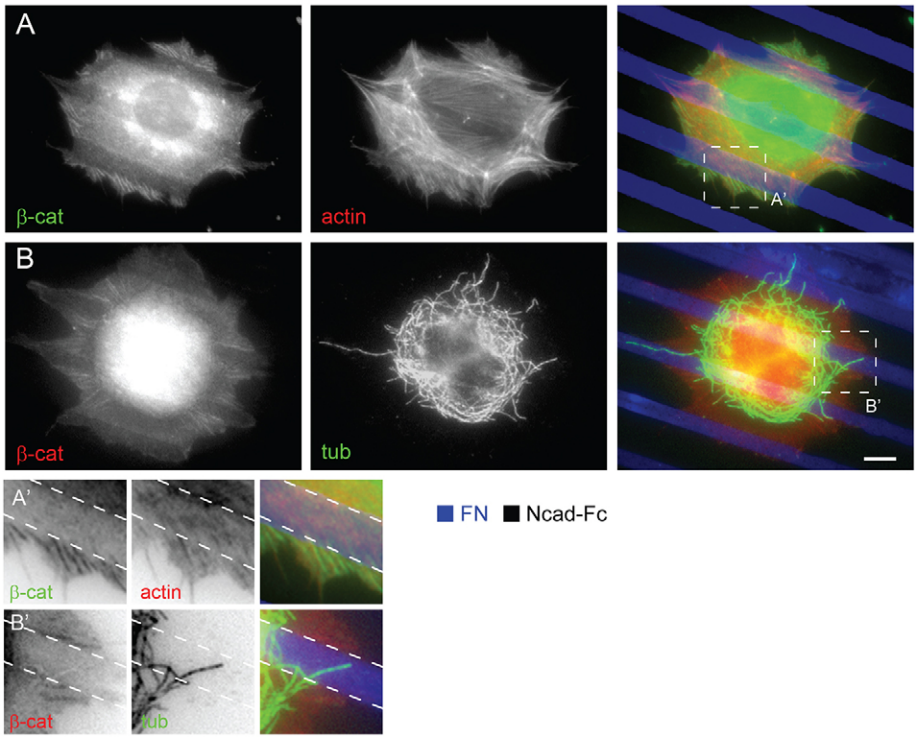

Fig. 2. Different effects of N-cadherin and integrin adhesions on F-actin and MT organizations. C2C12 cells were grown for 2 h on micropatterned substrates formed from alternating stripes of FN (blue) and Ncad–Fc (black), and then were fixed. Cells were immunostained for β-catenin (β-cat, green) and actin (red) (A,A′) or for β-catenin (red) and MTs (tub, green) (B,B′). Higher magnifications of the areas delimited by white dotted squares in A and B are represented in A′ and B′, respectively (inverted look-up tables); the position of FN stripes are shown by dotted lines in A′ and B′. Cells form N-cadherin adhesions, with β-catenin colocalizing with the actin cytoskeleton specifically over Ncad–Fc stripes (A,A′). Cells tend to produce longer protrusions on FN than on Ncad–Fc. MTs avoid regions of spreading on Ncad–Fc and preferentially invade areas adhering to FN (B,B′). Scale bar: 10 μm.

exert some kind of destabilizing and/or repulsive effects on MT plus ends.

The poor recruitment of MTs to the vicinity of cadherin adhesions might result from impaired elongation of MT plus ends, mis-orientation of growing MT plus ends or a combination of the two. To test the first hypothesis, we evaluated the effect of N-cadherin engagement on MT dynamics in living cells. End binding (EB) proteins, like other +TIPs, concentrate in comet-like structures at the plus ends of MTs during the MT polymerization phase, whereas they shuttle to the cytoplasm when MTs depolymerize (Stepanova et al., 2003). We first labeled growing plus ends by immunostaining for EB1 (also known as MAPRE1) in fixed confluent cell monolayers. MTs were oriented with their plus ends directed towards the cell–cell contacts (supplementary material Fig. S3A). Double immunostaining of MTs and MT plus ends in cells spread on Ncad–Fc or FN revealed that MTs were directed by their plus ends towards the cell periphery, which contained adhesion plaques (supplementary material Fig. S3B). In order to determine the localization of growing plus ends relative to these adhesion plaques, we performed EB1 immunostaining on fixed cells expressing either DsRed-tagged N-cadherin or GFP–vinculin that were spread on Ncad–Fc and FN, respectively (Fig. 3A). In accordance with the MT distribution, EB comets were very sparse in the peripheral zone of cells spread on Ncad–Fc, where cadherin adhesions are preferentially located. By contrast, EB comets were significantly more frequent at the edge of cells seeded on FN (Fig. 3B).

In order to follow MT dynamics, +TIP complexes were labeled in living cells by the expression of GFP-tagged EB1 or EB3 (also known as MAPRE3) proteins (supplementary material Movies 1,2). The movement of the EB comets was oriented towards the cell periphery, as expected. However, the persistence of these +TIP comets was significantly reduced in cells spread on Ncad–Fc compared with cells seeded on FN, suggesting that there was an overall reduced MT growth rate in these cells (Fig. 4A). To quantify this effect, EB-labeled comets were tracked, and their mean displacement velocity was calculated to give a proxy measurement of MT growth rate. The mean displacement rate of +TIP comets in lamellipodial areas was significantly lower on Ncad–Fc than on FN (Fig. 4B), suggesting that MT plus ends grow more slowly and/or undergo more frequent catastrophes on Ncad–Fc than on FN. We then quantified the relative accumulation of EB1–GFP in comets. EB proteins specifically associate with growing MT plus ends, thereby preventing catastrophes (Komarova et al., 2009), and their accumulation is thus expected to reflect the overall stability of MT plus ends. Accordingly, we observed a significant reduction in the area, elongation and labeling intensity of EB comets associated with MTs in the lamellipodia of cells seeded on Ncad–Fc compared with cells spread on FN (Table 1), indicating that less EB protein is associated with MT plus ends in cells seeded on Ncad–Fc, and thus that these MT plus ends are destabilized compared with those in cells seeded on FN.

In order to assess whether the reduction in MT growth rate was due to an inhibitory effect of N-cadherin engagement or to the absence of a positive signal provided by cell adhesion on FN, we perturbed N-cadherin signaling by overexpressing a truncated form of N-cadherin in which the ectodomain was deleted [DN-Ncad (Riehl et al., 1996)]. This construct has been reported to interfere with cadherin function, likely by competing for binding to β-catenin, thus lowering the stability of both cadherin and β-catenin in a dose-dependent manner (Bard et al., 2008; Taniguchi et al., 2006). The expression of DN-Ncad resulted in a comet displacement rate comparable to the one observed in cells spread on FN (Fig. 4B), indicating that the reduced MT growth rate observed on N-cadherin resulted from an inhibitory effect of cadherin signaling, rather than from the absence of a positive signal elicited by integrin activation. Thus, the prevention of MT penetration into the adhesion areas that is induced by N-cadherin

Journal of Cell Science (2014) 127, 1660–1671 doi:10.1242/jcs.131284

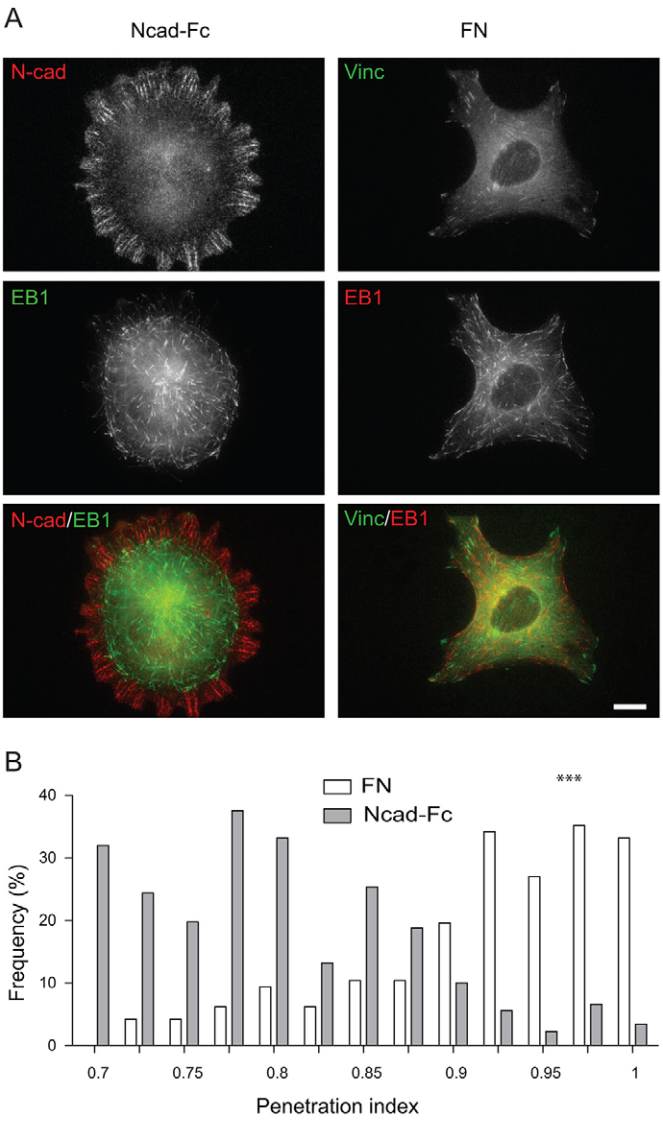

Fig. 3. Distribution of EB comets in cells spread on Ncad–Fc and FN. Cells expressing either DsRed–N-cadherin or GFP–vinculin (Vinc) were spread for 2 h on Ncad–Fc and FN, respectively. Fixed preparations were then immunostained for endogenous EB1. Shown are representative images (A) and quantitative analysis of the distribution of EB1 comets (B) in cells spread on Ncad–Fc and FN substrates. Scale bar: 10 µm. The relative position of individual comets was quantified in the distal third of the cell. The penetration index was defined as the measured distance of the comet from the cell centroid divided by the distance between the lamellipodial edge and the centroid of the cell along a line crossing the comet. The quantification was performed over three independent experiments, with five cells per condition and ~15 comets per cell. ***$P<0.0001$ (chi-square test).

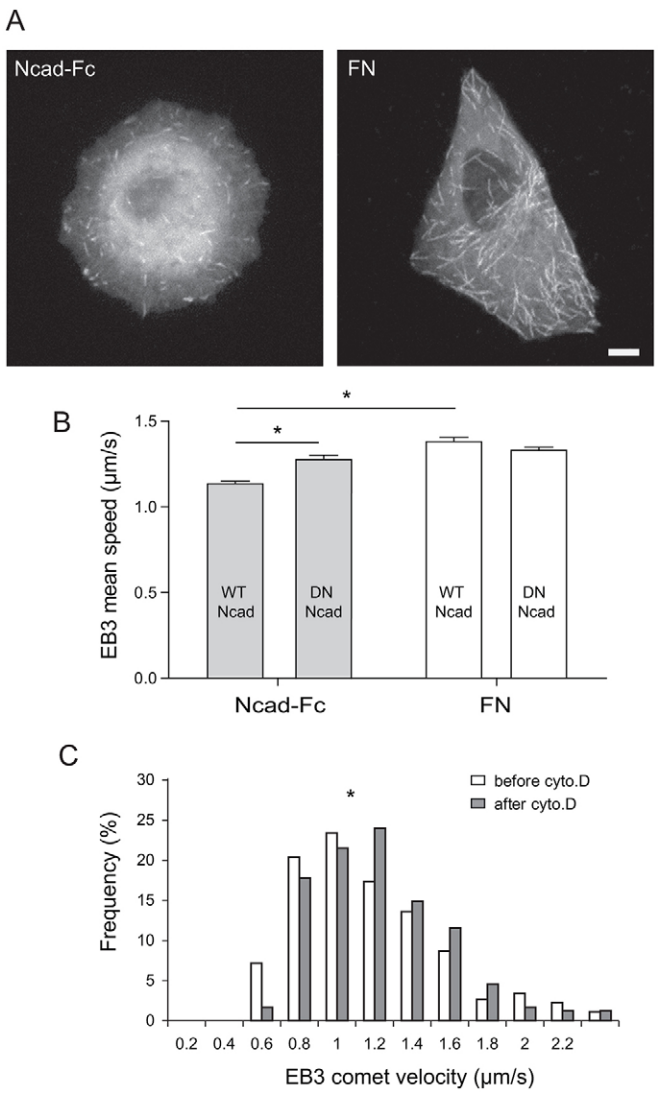

Fig. 4. EB3 comet persistence and MT mean growth rate are negatively regulated by cadherin engagement. Live-cell imaging was performed on EB3–GFP- or EB3–mCherry-expressing cells plated on Ncad–Fc and FN substrates. (A) Representative images of EB3 comet persistence were obtained by maximal projection of video frames (60 frames acquired over 15 s). Scale bar: 10 µm. (B) Cells expressing EB3–GFP and either wild-type N-cadherin or DN-Ncad fused to DsRed were plated onto Ncad–Fc and FN substrates and processed for live-cell imaging. The mean displacement speeds of MT +TIPs were significantly lower in the lamellipodia of cells seeded on Ncad–Fc than in the lamellipodia of those spread on FN. This inhibition was alleviated by the expression of the DN-Ncad mutant. The data show the means±s.e.m. (C) The mean displacement speeds of lamellipodial MT +TIPs were determined in cells spread on Ncad–Fc before and 20 min after treatment with 100 nM cytochalasin D. Results are expressed as the distribution of the mean displacement speeds of EB3 comets analyzed in three independent experiments, five cells per condition, 20 comets tracked per cell. *$P<0.05$ (non-parametric Mann–Whitney test).

engagement is accompanied by a significant reduction in MT growth rate, although no direct relationship between these two processes could be made from these observations.

Because, on the one hand, both cadherin and integrin receptors are linked to, and regulate, actin filaments, and, on the other, actin and MT networks have been reported to display both structural and regulatory interactions (Rodriguez et al., 2003), we hypothesized that MT dynamics and/or growth into cadherin adhesions might be regulated by the actin cytoskeleton. Thus, we analyzed the influence of actin filament depolymerization on the mean velocity of EB-labeled comets in cells seeded on Ncad–Fc (supplementary material Movie 3). We observed a significant but moderate shift in the distribution of EB comet velocities to higher values after treatment of cells with 100 nM cytochalasin D (Fig. 4C), indicating that the actin networks might indeed be involved in the inhibitory effect of N-cadherin engagement on MT dynamics. Taken together, these observations link MT growth in the vicinity of cadherin adhesions to cadherin signaling and the actin

Journal of Cell Science (2014) 127, 1660–1671 doi:10.1242/jcs.131284

Table 1. Morphological analysis of EB1 comets in cells plated on Ncad–Fc and fibronectin substrates

	Mean parameters of EB1 comets (±s.e.m.)			
	Area (μm^2)	Major axis (μm)	Circularity	Integrated density
Ncad–Fc (n=2803)	0.18±0.002	0.69±0.006	0.784±0.003	174.5±3.2
FN (n=5358)	0.19±0.002	0.74±0.005	0.721±0.003	224.3±1.2
P value	<0.005	<0.0001	<0.0001	<0.0001

C2C12 cells were cultured on Ncad–Fc or fibronectin (FN) substrates for 2 h, and then were immunostained for β-catenin and EB1. The analysis of EB1 comet morphology was performed with the help of ImageJ software after manual thresholding by measuring the area, the major axis length, the circularity and the integrated density of comets located in the distal region of the lamellipodia. The comets formed on N-cadherin substrates are smaller, more circular and less dense than the ones formed by cells on fibronectin.

cytoskeleton, although they do not explain the molecular mechanisms that prevent MTs from reaching cadherin adhesions.

The actin network is responsible for the inhibition of MT recruitment to cadherin adhesions

Given the results reported above, we hypothesized that MT penetration might be counteracted by actin treadmilling occurring in the opposite direction to MT growth at the cell periphery (Ponti et al., 2004). Alternatively, MTs might be physically blocked by the actin network, as suggested by previous reports on the negative effect of actomyosin contractile bundles on the growth of MTs into neuronal growth cones (Burnette et al., 2007; Dent et al., 2007). To address these issues, we studied the impact of cadherin engagement on actin retrograde flow. Actin dynamics were visualized by using the LifeAct probe (Riedl et al., 2008) in cells seeded either on Ncad–Fc or FN (supplementary material Movies 5,6), and the actin treadmilling speed was quantified by kymograph analysis (Fig. 5A). We observed a twofold higher actin retrograde flow in cells spread on N-cadherin compared with cells spread on FN. Thus, the reduced growth of MTs into N-cadherin adhesions compared with FN adhesions correlates with increased actin dynamics. In order to test for a functional link between actin retrograde flow and MT penetration, we treated LifeAct-expressing cells with the myosin II inhibitor blebbistatin. Blebbistatin treatment drastically reduced the rearward movement of actin filaments (Fig. 5B). However, in contrast to cytochalasin treatment, treatment of cells with blebbistatin induced a moderate reduction in MT growth rate (supplementary material Movie 4). This result is not consistent with the hypothesis that MT plus end penetration is merely

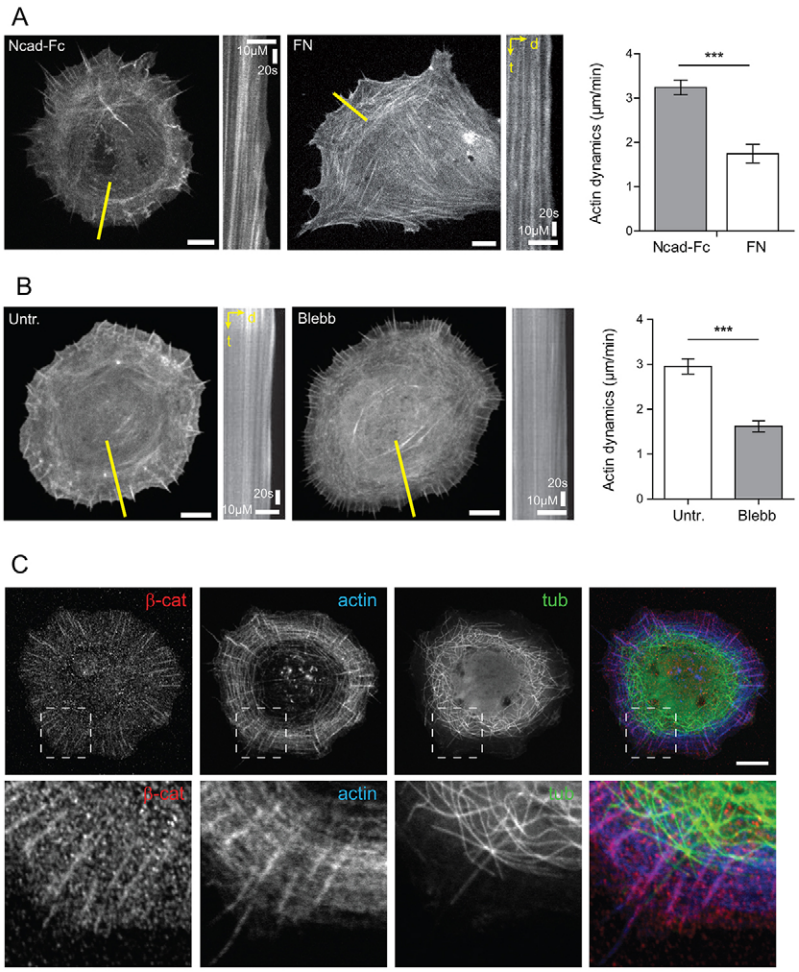

Fig. 5. N-cadherin engagement stimulates the actin retrograde flow. (A) Cells coexpressing LifeAct–GFP and N-cadherin–DsRed were plated on either Ncad–Fc or FN, and were subjected to live-cell imaging. The actin retrograde flow was quantified by kymograph analysis on regions located in the lamellipodium over the adhesion areas (yellow lines). The actin retrograde flow was significantly faster for cells seeded on Ncad–Fc than for cells seeded on FN. (B) Similar live-cell imaging and analysis were performed for cells seeded on Ncad–Fc in the absence of treatment (Untr.) or after a 20 min treatment with 20 μM blebbistatin (Blebb). The data show the means±s.e.m. ***P<0.0001 (Student's t-test, three independent experiments). (C) Cells plated on Ncad–Fc for 2 h were fixed and analyzed for the distribution of β-catenin (β-cat, red), F-actin (blue) and α-tubulin (tub, green). The areas delimited by white dotted squares is shown at higher magnification (lower panels). Note that most of the MTs were oriented tangentially to the circular actin filament bundle at the rear of cadherin adhesions. Scale bars: 10 μm.

Journal of Cell Science (2014) 127, 1660–1671 doi:10.1242/jcs.131284

slowed down by the flow of actin filaments in the opposite direction (Ponti et al., 2004). In addition, the expression of a DN-Ncad, which rescues the inhibitory effects of N-cadherin engagement on MT growth dynamics, had no effect on the growth of MTs into cadherin adhesions (supplementary material Fig. S4), suggesting that the reduced MT growth rate observed on Ncad–Fc might not be the cause of the limited penetration of MT plus ends into cadherin adhesion areas.

A more precise analysis of the distribution of MTs and actin filaments revealed that most of the MTs did not pass through the tangential actomyosin arc present at the rear of the lamellipodium but, instead, turned tangentially along these actin filaments (Fig. 5C). The orientation of EB-labeled plus ends was consistent with these observations (Fig. 3; supplementary material Fig. S3). These observations suggest that the contractile actomyosin arc formed at the rear of cadherin adhesions might relay the inhibition of MT penetration. To test this hypothesis, we analyzed the effect of cytochalasin treatments on the penetration of MTs (Fig. 6A). Mild actin disruption with cytochalasin B significantly increased the growth of MTs into the area containing cadherin adhesions. Treatment with cytochalasin D, a much more potent inhibitor of actin polymerization, induced a drastic disruption of the actin network (supplementary material Fig. S5) and triggered the full penetration of MTs into the lamellipodia of cells seeded on N-cadherin (Fig. 6A). This result supports the notion that the circular actin bundles at the rear of the lamellipodia have an obstructive effect on MT growth into the vicinity of cadherin adhesions. To further test this hypothesis, we treated the cells with blebbistatin to independently disrupt this contractile structure. Blebbistatin treatments indeed disrupted the contractile actomyosin ring (supplementary material Fig. S5), and significantly increased the penetration of MTs into the lamellipodium (Fig. 6B), indicating that the actomyosin network that is organized at the rear of cadherin adhesions is the principal element preventing MT targeting to cadherin adhesions. Taken together, these results reveal an obstructive effect of the tangential actin bundles on MT penetration into the adhesion area that is independent of the modulation of MT growth.

Perturbation of MT dynamics stabilizes N-cadherin adhesion

We next asked whether the limited penetration of MTs into the vicinity of cadherin adhesions and their altered dynamics in the

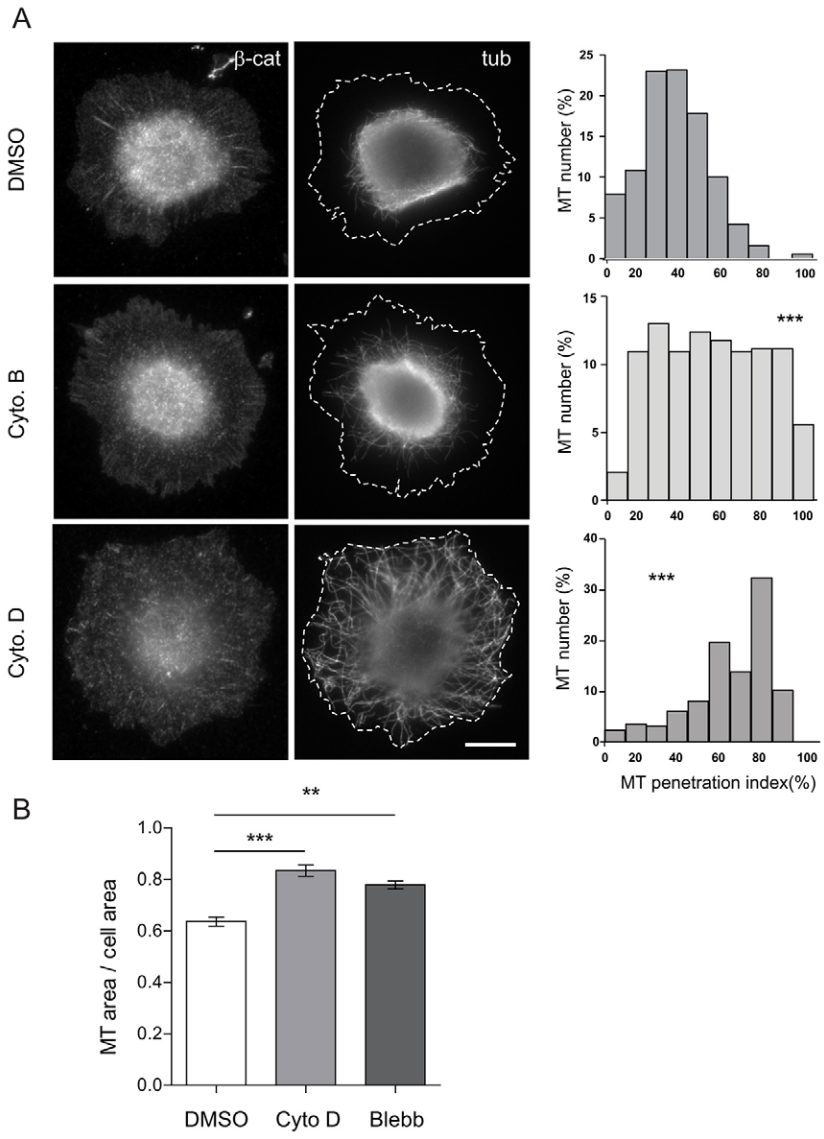

Fig. 6. An actomyosin belt is responsible for the inhibition of MT recruitment to cadherin adhesions. (A) Cells plated for 2 h on Ncad–Fc were treated with DMSO, cytochalasin B (Cyto. B, 350 nM) or cytochalasin D (Cyto. D, 100 nM) for 20 min before fixation and staining for β-catenin (β-cat, left) and α-tubulin (tub, right). The dotted line shows the outline of the cell. A penetration index in the lamellipodium was measured for individual MTs, defined as the ratio of the MT penetration distance into the lamellipodium divided by the depth of the lamellipodium. Under control conditions (DMSO), a large fraction of individual MTs weakly penetrated into the lamellipodium. Cytochalasin B and D treatments led to an increasing fraction of MTs fully penetrating into the lamellipodium. Scale bar: 10 μm. Quantification was performed over two independent experiments with ~200 MTs for each condition. ***$P<0.0001$ for both cytochalasin B and cytochalasin D compared with DMSO (non-parametric Mann-Whitney test). (B) Cells plated for 2 h on Ncad–Fc were treated with DMSO, cytochalasin D (100 nM) or blebbistatin (Blebb, 20 μM) for 20 min before fixation and evaluation of the spreading of the MT network, as reported for Fig. 1. Results are expressed as the means±s.e.m. from three independent experiments, $n \geq 16$ cells per condition. **$P<0.001$, ***$P<0.0001$ (one-way ANOVA test).

Journal of Cell Science (2014) 127, 1660–1671 doi:10.1242/jcs.131284

adhesion area might have an impact on the formation or stabilization of the adhesions. The pretreatment of cells with nocodazole (1 or 10 μM) or taxol (10 μM) had no significant effect on the capacity of C2C12 cells to adhere to the Ncad–Fc substrate (data not shown). After spreading on Ncad–Fc, treatment of the cells with nocodazole or taxol had no further destabilizing effect on preformed cadherin adhesions (Fig. 7A), confirming that MTs are not required for the formation and maintenance of N-cadherin-mediated adhesion plaques (Gavard et al., 2004). Because the depolymerization of MTs has been reported to increase contractility (Chang et al., 2008), cells were also treated with nocodazole at a lower concentration that has been reported to affect MT dynamics without depolymerizing the network (Vasquez et al., 1997). Treatment with the lower concentration of nocodazole had no significant effect on cadherin adhesions (data not shown). By contrast, quantification of the level of β-catenin accumulation in individual cadherin adhesions revealed that they contained significantly more cadherin–catenin complexes after taxol treatment (Fig. 7B). This positive effect on the recruitment of adhesion complexes was paralleled by a reduction in the penetration of taxol-stabilized MTs into the peripheral adhesion-rich area of the cells (Fig. 7C). Interestingly, short treatments of confluent cell cultures with taxol induced a significant increase in N-cadherin levels that could be detected in total protein extracts by western blotting (data not shown). This result is compatible with a stabilizing effect of this treatment on N-cadherin-mediated adhesions.

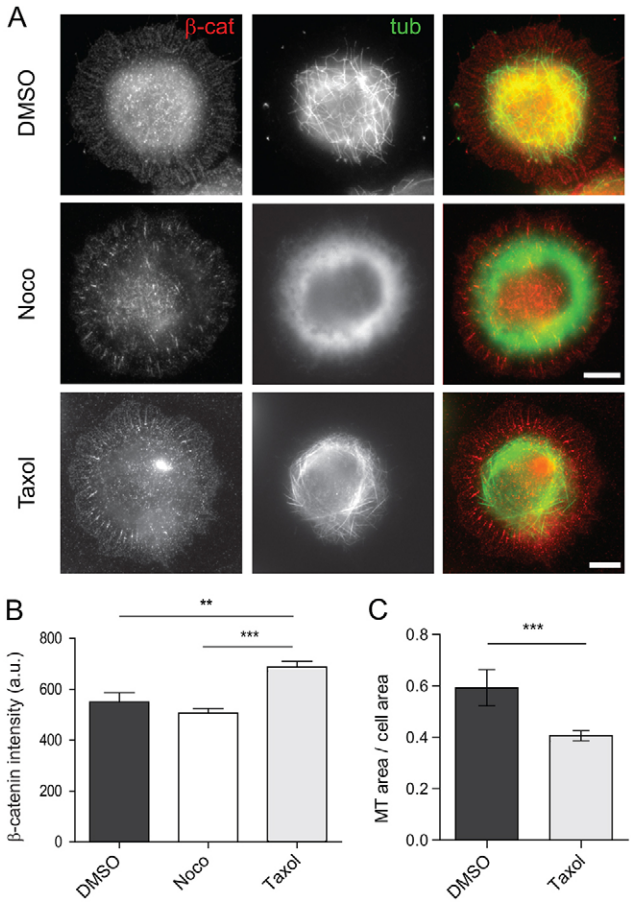

Fig. 7. Reduced dynamicity of MTs promotes the stabilization of N-cadherin adhesions. (A) Cells spread on Ncad–Fc were treated for 20 min with nocodazole (Noco, 10 μM), taxol (10 μM) or DMSO, and were then fixed and immunostained for β-catenin (β-cat, red) and α-tubulin (tub, green). MTs are depolymerized in nocodazole-treated cells and bundled in taxol-treated cells. Scale bars: 10 μm. (B) Quantification of the accumulation of β-catenin in cadherin adhesions was performed as described in Materials and Methods. Taxol treatment induced a significant increase in the amount of accumulated β-catenin. (C) Quantification of the effect of taxol on the distribution of MTs. The data show the means±s.e.m. from four independent experiments, $n \geq 16$ cells per condition. $^{**}P<0.001$, $^{***}P<0.0001$ (one-way ANOVA).

DISCUSSION

Through its dynamic orientation, growth and capture, the MT network is a major regulator of cell shape, cell polarization and migration. It is thought to direct these processes in part through regulation of cell–extracellular-matrix and cell–cell contacts. In particular, MT plus ends are targeted to focal adhesions, and the presence of the MTs has been reported to contribute to the destabilization of these anchoring junctions, which participate in the polarization of migrating cells (Small and Kaverina, 2003). In turn, the MT network might be instructed to polarize by cell–matrix and cell–cell adhesion plaques. However, the relationship between MTs and cell–cell contacts remains poorly understood, and our understanding is mostly limited to E-cadherin-mediated intercellular junctions in epithelial cells. Here, we analyzed the influence of N-cadherin engagement on MT recruitment and dynamics in myogenic cells. We found that: (1) although MTs are directed by their plus ends towards the cell periphery where adhesion sites are located, MTs are repelled from N-cadherin-mediated adhesion sites; (2) the mean elongation rate of MTs is reduced by N-cadherin engagement compared with FN-induced integrin engagement; (3) the prominent factor limiting the growth of MTs into cadherin adhesion areas is the presence of strong tangential actomyosin arcs formed at the rear of these adhesion areas, which induce MTs to turn; (4) this negative regulation of MT penetration at nascent contacts might be required to strengthen N-cadherin-mediated adhesions; (5) the resulting bias in MT recruitment to focal adhesions and cadherin adhesions (as illustrated by the distribution of MTs in cells spread on micropatterned substrates made of alternating stripes of N-cadherin and FN), and the subsequent regulation of cell-contact turnover might be a major factor in cell polarization.

We show here that MTs are directed towards N-cadherin-mediated contacts by their plus ends, and that they are involved in a negative-feedback loop with the formation of cell–cell contacts in myogenic cells. Although MTs can associate with adherens junctions through their minus ends in epithelial cells (Meng et al., 2008), the attraction and targeting of centrosomal MT plus ends to E-cadherin-mediated junctions have been linked to positive feedback on junctional stability (Ratheesh et al., 2012; Stehbens et al., 2006). These discrepancies might be related to differences in cadherin-specific signaling pathways, although N-cadherin is also able to mediate the formation of adherens junctions in some cell types (Radice et al., 1997). Indeed, cell–cell contact morphology, dynamics and stability are very different in epithelial and myogenic cells, the former presenting a fibroblastic phenotype with poorly differentiated cell–cell contacts that are devoid of true adherens junctions (Mège et al., 2006). By contrast, a negative-feedback loop has also been reported very recently between vascular-endothelial (VE)-cadherin-mediated contacts and MT growth in endothelial cells (Komarova et al., 2012). In addition, we observed that MTs were also repelled from cadherin adhesions formed by epithelial MDCK cells on an

Journal of Cell Science (2014) 127, 1660–1671 doi:10.1242/jcs.131284

E-cadherin–Fc substrate. Thus, MT repulsion might be a general feature of cadherin-mediated cell–cell contacts that could be overcome by other regulatory mechanims at epithelial cell–cell contacts.

Here, we focused on the different effects of N-cadherin-mediated versus integrin-mediated adhesion on MTs by using an approach that allowed us to dissociate the effects of the two types of receptors and, thus, to reveal specific pathways that are masked when both types of junctions are mixed in the culture system (Gavard et al., 2004). Accordingly, our data can be interpreted as showing preferential recruitment and increased growth rate of MTs at cell–extracellular-matrix contacts versus cell–cell contacts, in relation to the establishment of a front–rear cell polarity required for migration (Kadir et al., 2011). These data are consistent with previous observations of a clear bias of MT growth towards the free edge of cells at the border of cell islands (Dupin et al., 2009; Jaulin and Kreitzer, 2010). Thus, our observations are consistent with a major role for a balance between spatially segregated integrin and N-cadherin signaling in biasing MT distribution and dynamics. We propose that this bias is central to the polarization of the MT network, initiating the further polarization of organelles and the cell motility system that is required to initiate cell migration during development or during wound healing *in vitro*.

Our results support the hypothesis that the reduced MT dynamics at N-cadherin-mediated contacts results from an inhibitory action of N-cadherin engagement, rather than from the absence of a positive signal provided by integrins, as reported for VE-cadherin engagement (Komarova et al., 2012). Indeed, the reduction of MT growth rate can be alleviated by the expression of a truncated form of N-cadherin, which interferes with the function of this protein by sequestering catenins and thus destabilizing cadherin adhesion complexes. The reduction in MT growth upon N-cadherin engagement was associated with a significant reduction in the accumulation of EB proteins at MT plus ends, suggesting that N-cadherin engagement could promote the dissociation of these +TIPs from the MT plus ends. Although we have no knowledge of the exact signaling pathway involved, this process might be mediated by signaling proteins such as Src (Komarova et al., 2012) or Rho family GTPases, which are known to be activated by cadherin engagement and to modulate MT dynamics (Fukata et al., 2003; Stehbens et al., 2009). MT dynamics might also rely on cell contractility, as suggested by the effect of blebbistatin treatment, consistent with the recently reported modulation of MT growth in endothelial cells by myosin-II-mediated mechanosensing on fibronectin (Myers et al., 2011). Alternatively, by using co-immunoprecipitation, we detected the association of the +TIPs EB1, EB3 and CLIP115 with catenins (data not shown), as reported previously for EB proteins in myogenic cells (Straube and Merdes, 2007; Zhang et al., 2009). These results suggest that the destabilization of +TIP complexes might result from direct interactions of some of their components with cadherin-associated proteins.

However, our major finding is that MT plus ends are kept at a distance from cadherin adhesions, whereas they are targeted to focal adhesions. The fact the expression of DN-Ncad has no effect on MT distribution suggests that the effect of N-cadherin on MT penetration and on plus-end dynamics might be independent of N-cadherin signaling and/or is not mediated at the same threshold of N-cadherin signaling. The major obstacle to MT penetration into areas containing cadherin adhesions was not the reduction in the stability of plus ends and polymerization, but, instead, seemed to be the physical barrier formed by circular actin cables at the rear of the adhesion area. Indeed, in cells seeded on FN, it has been shown that MTs are guided along stress fibers to reach the leading edge (Huda et al., 2012). By contrast, cells on Ncad–Fc do not form longitudinal stress fibers but, instead, have actin filaments that are organized in a circular dense actomyosin belt. This might explain why MTs do not reach N-cadherin adhesions, whereas they are targeted to focal adhesions as reported by Kaverina and colleagues (Kaverina et al., 1998).

The organization of actomyosin into tangential bundles is a common form of self-organization of actin filaments in spreading cells, which is independent of the nature of the adhesion signal (Gavard et al., 2004; Prager-Khoutorsky et al., 2011; Zamir et al., 2000). It might result from the continuous flow and severing of the branched network of actin filaments that elongate at the lamellipodial leading edge (Craig et al., 2012). On FN substrates, following the reinforcement of focal adhesions that are subjected to sustained increased contractility, cells shift their actin organization from an isotropic actomyosin belt to stress fibers, initializing cell polarization (Prager-Khoutorsky et al., 2011; Zamir et al., 2000). As reported previously, this shift in actin organization never occurs in cells seeded on N-cadherin, even at longer time scales. Consequently, cells are non-motile and their actin remains organized in concentric actomyosin rings (Gavard et al., 2004). Thus, the formation of actomyosin arcs seems to be a ‘default’ organization of actin that is common to both N-cadherin and integrin activation. Integrins further signal to switch this actin organization to longitudinal stress fibers (Prager-Khoutorsky et al., 2011). Such a symmetry-breaking mechanism on FN-coated substrates depends on substrate stiffness (Trichet et al., 2012) and thus on cell-generated traction forces. The amplitude of forces exerted on N-cadherin-coated substrates is lower than that on FN (Ladoux et al., 2010). Furthermore, the actin treadmilling speed is higher on N-cadherin than on FN, which could be interpreted as a lower degree of coupling of N-cadherin to actin filaments (Craig et al., 2012; Giannone et al., 2009). As a result, cadherin adhesions would not initiate or tolerate the increased internal cell tension required for actin reorganization.

Indeed, we report here for the first time that the lamellipodial retrograde actin flow is two times faster following N-cadherin engagement than following integrin engagement. We cannot exclude the possibility that this stimulation is associated with the sequestration of α-catenin by cadherins at nascent contacts, alleviating the inhibitory effect of the free pool of dimeric α-catenin on Arp2/Arp3-complex-mediated actin polymerization (Benjamin et al., 2010). This increased actin treadmilling could be causal in the formation of the strong tangential actomyosin belt. More likely, this increased treadmilling speed reflects a weaker anchorage of cadherin to actin filaments, which is consistent with the reduced lamellipodial spreading of cells on N-cadherin-coated versus FN-coated stripes (Fig. 2), and with the results of the direct measurement of tensile forces developed by cells on alternating stripes of E-cadherin and collagen (Borghi et al., 2010). The lower tensile properties of N-cadherin adhesion might prevent the rupture of the tangential actomyosin belt, which is responsible for MT exclusion from the adhesion zone. Interestingly, it has been reported very recently that actin filaments and myosin II are polarized towards cadherin mediated cell–cell contacts in cell doublets seeded on lines of FN (Ouyang et al., 2013). Although the actomyosin belt is not obvious at actual cell–cell contacts, a similar structure has been seen clearly during cell–cell contact maturation

(Adams et al., 1996; Ivanov et al., 2006; Ivanov et al., 2004) and might thus represent a general structural trait of cell–cell contacts.

These results functionally link the engagement of N-cadherin and the organization of actin at nascent cell–cell contacts to the repulsion of MTs. We found that the alteration of MT dynamics and the compaction of the MT network induced by taxol stimulates the recruitment of cadherin complexes to adhesion plaques. Nocodazole-induced MT depolymerization did not change the capacity of the cells to form and maintain their adhesions, confirming that MTs are not necessary for the formation of cadherin adhesions once the N-cadherin molecules have reached the plasma membrane (Gavard et al., 2004). This is in contrast to results obtained in epithelial cells, where MT integrity is important for the establishment and maintenance of cell–cell junctions (Ligon and Holzbaur, 2007; Ratheesh et al., 2012; Stehbens et al., 2006; Waterman-Storer et al., 2000). However, other studies report that cadherin contacts are negatively regulated by MTs in epithelial and endothelial cells (Ivanov et al., 2006; Kee and Steinert, 2001; Komarova et al., 2012; Lorenowicz et al., 2007). Although further studies will be required in order to understand the effects of MTs in the vicinity of cell–cell contacts, the present work suggests that, in myogenic cells at least, the negative regulation of MTs at nascent N-cadherin-mediated contacts promotes the strengthening of intercellular adhesions.

Taken together, these results clearly establish cadherins, actin filaments and the MTs as inter-regulated partners that play an essential role in establishing front–rear cell polarity. At the center of this regulatory loop, we demonstrate that N-cadherin engagement negatively regulates the dynamics of MTs through as-yet-unknown outside-in signaling, and negatively regulates the recruitment of MTs through the stimulation of actin dynamics and the organization of tangential actomyosin arcs. We propose that this regulation is instrumental in the polarization of organelles and the cell motility system that is required for front–rear polarization associated with cell migration during developmental or wound healing processes.

MATERIALS AND METHODS

Cell culture and electroporation

Mouse myogenic C2C12 and MDCK cells were grown in Dulbecco's modified Eagle's medium (DMEM) containing 10% fetal calf serum (FCS) and 100 IU/ml of penicillin-streptomycin at 37℃ under 5% CO_2. Cells were electroporated with the Equibio Easyject Plus electroporator (Wolf Laboratories), using the following conditions: 5×10^6 cells, 30 µg of expression vector in 15 mM HEPES pH 7.2, 260V, 1600F.

Plasmids, antibodies, drugs and Ncad–Fc protein

The EB3–GFP construct was obtained from Florence Niedergang (Institut Cochin, Paris, France). The EB1–GFP and EB3–mCherry constructs were obtained from Annie Andrieux (Institut des Neurosciences, Grenoble, France) (Efimov et al., 2008; Peris et al., 2006). The LifeAct–GFP and DN-Ncad constructs were described previously (Riedl et al., 2008; Lelièvre et al., 2012, respectively). The antibodies used in this study were: rabbit polyclonal anti-β-catenin (Sigma), anti-Glu-tubulin [recognizing detyrosinated α-tubulin (AbCys)], monoclonal anti-N-cadherin (Zymed), anti-EB1 (BD Biosciences), anti-α-tubulin (Sigma), anti-acetylated-α-tubulin (Sigma) and anti-tyrosinated α-tubulin (Sigma). Alexa-Fluor-643–phalloidin was obtained from Molecular Probes. Where indicated, cells were treated for 20 min with the following drugs at the indicated concentration: cytochalasin B (Sigma), cytochalasin D (Fluka), blebbistatin (Calbiochem), nocodazole (Sigma) and taxol (Sigma). The recombinant Ncad–Fc protein was produced in HEK-293 cells and purified on Protein-G-coupled Sepharose (Fast flow, GE Healthcare) according to established protocols (Lambert et al., 2000).

Substrate coating and cell-spreading assays

Cleaned silanized glass coverslips were coated with either fibronectin or Ncad–Fc, as described previously (Gavard et al., 2004). For micropattern printing, polydimethylsiloxane (PDMS) stamps were prepared by pouring a PDMS solution (Sylgard, Dow Corning) onto a 'wafer' and allowing it to polymerize at 60℃ overnight (Ganz et al., 2006). The PDMS stamps were pulled off and incubated face up for 45 min at room temperature, with a mixture of fibronectin and Cy3-conjugated IgG. After several washes with deionized water, the stamps were dried and applied onto silanized glass coverslips, then the printed areas were blocked with 3% BSA, 0.2% Pluronic (Life Technologies) for 1 h at room temperature. For mixed micropatterns composed of fibronectin and Ncad–Fc stripes, fibronectin-stamped coverslips were incubated with anti-Fc antibody (Jackson ImmunoResearch) overnight at 4℃, then with recombinant Ncad–Fc for 2 h at room temperature before the blocking step. Cells that had been mechanically dissociated in cold PBS plus 1.5% BSA and 3.5 mM EDTA were then plated onto the different substrates at 2×10^4 cells/cm^2, and were incubated for 2 h at 37℃ under 5% CO_2 for classical substrates, and overnight for the micropatterns.

Immunofluorescent staining

For most staining experiments, cells were fixed for 15 min with PBS that was pre-warmed to 37℃, and contained 4% formaldehyde and 0.33 M sucrose. For +TIP staining experiments, cells were fixed for 10 min with methanol that was pre-chilled to −20℃. Fixed preparations were permeabilized with a solution of 0.15% Triton X-100 in PBS for 5 min, and were saturated with 1.5% BSA in PBS for 1 h, then incubated with primary antibodies in PBS plus 1.5% BSA for 2 h at room temperature. The samples were incubated with secondary antibodies (Jackson Laboratories) for 1 h, or with Alexa-Fluor-647-phalloidin (Molecular Probes) for 45 min for actin labeling. The preparations were observed by using confocal microscopy (Fv10i, Olympus; SP5, Leica) or by using an epifluorescence microscope (DM 6000 Leica) with a 63× objective, and images were captured with a Micromax CCD camera (Roper Scientific) driven by the MetaMorph software.

Spinning-disk acquisitions

The culture medium was replaced 30 min before acquisition with DMEM-F12 medium (Gibco) containing 10 mM HEPES, 0.54% glucose, 2 mM glutamine and 2 mM sodium pyruvate. Acquisitions were performed by using a Leica DMI4000 inverted microscope (with a 63× objective) coupled to a spinning-disk confocal module (CS20 head, Yokogawa) and an intensified CCD camera (Quantem S12SC, Roper Scientific), driven by MetaMorph. Images were acquired every 100 or 500 ms at the excitation wavelengths 491 and 561 nm, with an exposure time of 100 ms. The temperature was maintained at 37℃ by using a temperature-controlled chamber (Life Imaging).

Image analysis

All quantitative image analyses were performed by using NIH ImageJ software, and statistics were performed by using the GraphPad Prism software. The surfaces that were occupied by MTs were determined in preparations of cells stained for both β-catenin and tyrosinated tubulin. Acquired images were thresholded, then binarized to extract the surface occupied by the cell (β-catenin staining) and the MT networks (tubulin staining). Quantification was performed over three independent experiments with around ten cells for each condition. For the determination of the mean speed displacement of +TIP comets, instantaneous displacements were determined frame by frame (with acquisition every 500 ms to 1 s) by manual tracking of the EB3 comets using the MTrackJ plug-in (Meijering et al., 2012). The mean speed displacements were calculated for each comet over ~5–10 frames. Owing to the fact that the very poor signal:noise ratio of EB3 comets in the center of cells seeded on Ncad–Fc impeded tracking, the quantification was limited to the lamellipodia of cells seeded on both

Ncad–Fc and FN substrates. Quantifications were performed over three independent experiments, with five cells and 20 comets per cell. For analysis of actin dynamics, spinning-disk acquisitions were performed on cells expressing LifeAct–GFP. The mean speed of the actin retrograde flow was extracted by constructing kymographs over 1-pixel-broad lines drawn in regions of interest, giving a representation of the displacement of the fluorescent signal over time. All the lines that were detectable by eye were considered, and their slopes were determined manually by tracing over a straight line using ImageJ. For the quantification of β-catenin accumulation, β-catenin-labeled cadherin adhesion structures were manually thresholded by using ImageJ to identify their contour. The corresponding mask was applied to the original image after background subtraction, to extract the mean fluorescence intensity of the β-catenin signal within these structures for a given cell.

Acknowledgements
R.M.M. is a CNRS Research Director fellow. Fixed- and live-cell imaging was performed in the Institut du Fer à Moulin Cell Imaging Facility. We thank Annie Andrieux and Florence Niedergang for providing EB-tagged expression vectors, and André Sobel (Institut du Fer à Moulin, Paris, France) for critical reading of the manuscript. We also thank Laurence Duchesne (Université Rennes I, Rennes, France) for her help in optimizing Ncad–Fc production and purification. We would like to thank Théano Irinoipoulou (Institut du Fer à Moulin) for her help in statistics.

Competing interests
The authors declare no competing interests.

Author contributions
C.P. contributed to the design of the experiments, performed most of the experiments and helped in writing of the manuscript; P.-O.S. performed part of the actin dynamics and patterned substrate experiments, and contributed to the quantitative analysis of some of the other data, as well as to discussions; R.S. performed alternated stripes experiments and participated to discussions. E.N. performed experiments with MDCK cells; B.L. supervised patterning and participated to discussions and manuscript corrections; R.-M.M. directed the work and wrote the manuscript.

Funding
This work was supported by the Centre National de la Recherche Scientifique (CNRS); the Institut National de la Santé et de la Recherche Médicale (INSERM); and by grants from the Association Française de Recherche sur le Cancer (ARC); Association Française contre les Myopathies (AFM); the Agence Nationale de la Recherche ANR Blanc program MECANOCAD [grant number ANR-10-02]; and the Human Frontier Science Program (HFSP) [grant number RGP0040/2012]. C.P. was supported by a Ministère de la Recherche PhD fellowship, then by an ARC fellowship. P.-O.S. was supported by an ANR fellowship [grant number ANR-10-02]. R.S. was supported by a C'Nano program Région Ile de France doctoral fellowship.

Supplementary material
Supplementary material available online at
http://jcs.biologists.org/lookup/suppl/doi:10.1242/jcs.131284/-/DC1

References
Adams, C. L., Nelson, W. J. and Smith, S. J. (1996). Quantitative analysis of cadherin-catenin-actin reorganization during development of cell-cell adhesion. *J. Cell Biol.* **135**, 1899-1911.
Bacallao, R., Antony, C., Dotti, C., Karsenti, E., Stelzer, E. H. and Simons, K. (1989). The subcellular organization of Madin-Darby canine kidney cells during the formation of a polarized epithelium. *J. Cell Biol.* **109**, 2817-2832.
Bard, L., Boscher, C., Lambert, M., Mège, R. M., Choquet, D. and Thoumine, O. (2008). A molecular clutch between the actin flow and N-cadherin adhesions drives growth cone migration. *J. Neurosci.* **28**, 5879-5890.
Benjamin, J. M., Kwiatkowski, A. V., Yang, C., Korobova, F., Pokutta, S., Svitkina, T., Weis, W. I. and Nelson, W. J. (2010). AlphaE-catenin regulates actin dynamics independently of cadherin-mediated cell-cell adhesion. *J. Cell Biol.* **189**, 339-352.
Borghi, N., Lowndes, M., Maruthamuthu, V., Gardel, M. L. and Nelson, W. J. (2010). Regulation of cell motile behavior by crosstalk between cadherin- and integrin-mediated adhesions. *Proc. Natl. Acad. Sci. USA* **107**, 13324-13329.
Boscher, C. and Mège, R. M. (2008). Cadherin-11 interacts with the FGF receptor and induces neurite outgrowth through associated downstream signalling. *Cell. Signal.* **20**, 1061-1072.
Burnette, D. T., Schaefer, A. W., Ji, L., Danuser, G. and Forscher, P. (2007). Filopodial actin bundles are not necessary for microtubule advance into the peripheral domain of Aplysia neuronal growth cones. *Nat. Cell Biol.* **9**, 1360-1369.
Chang, Y. C., Nalbant, P., Birkenfeld, J., Chang, Z. F. and Bokoch, G. M. (2008). GEF-H1 couples nocodazole-induced microtubule disassembly to cell contractility via RhoA. *Mol. Biol. Cell* **19**, 2147-2153.
Chausovsky, A., Bershadsky, A. D. and Borisy, G. G. (2000). Cadherin-mediated regulation of microtubule dynamics. *Nat. Cell Biol.* **2**, 797-804.
Chen, X., Kojima, S., Borisy, G. G. and Green, K. J. (2003). p120 catenin associates with kinesin and facilitates the transport of cadherin-catenin complexes to intercellular junctions. *J. Cell Biol.* **163**, 547-557.
Craig, E. M., Van Goor, D., Forscher, P. and Mogilner, A. (2012). Membrane tension, myosin force, and actin turnover maintain actin treadmill in the nerve growth cone. *Biophys. J.* **102**, 1503-1513.
Dent, E. W., Kwiatkowski, A. V., Mebane, L. M., Philippar, U., Barzik, M., Rubinson, D. A., Gupton, S., Van Veen, J. E., Furman, C., Zhang, J. et al. (2007). Filopodia are required for cortical neurite initiation. *Nat. Cell Biol.* **9**, 1347-1359.
Desai, R. A., Gao, L., Raghavan, S., Liu, W. F. and Chen, C. S. (2009). Cell polarity triggered by cell-cell adhesion via E-cadherin. *J. Cell Sci.* **122**, 905-911.
Dupin, I., Camand, E. and Etienne-Manneville, S. (2009). Classical cadherins control nucleus and centrosome position and cell polarity. *J. Cell Biol.* **185**, 779-786.
Efimov, A., Schiefermeier, N., Grigoriev, I., Ohi, R., Brown, M. C., Turner, C. E., Small, J. V. and Kaverina, I. (2008). Paxillin-dependent stimulation of microtubule catastrophes at focal adhesion sites. *J. Cell Sci.* **121**, 196-204.
Franco, S. J., Martinez-Garay, I., Gil-Sanz, C., Harkins-Perry, S. R. and Müller, U. (2011). Reelin regulates cadherin function via Dab1/Rap1 to control neuronal migration and lamination in the neocortex. *Neuron* **69**, 482-497.
Fukata, M., Watanabe, T., Noritake, J., Nakagawa, M., Yamaga, M., Kuroda, S., Matsuura, Y., Iwamatsu, A., Perez, F. and Kaibuchi, K. (2002). Rac1 and Cdc42 capture microtubules through IQGAP1 and CLIP-170. *Cell* **109**, 873-885.
Fukata, M., Nakagawa, M. and Kaibuchi, K. (2003). Roles of Rho-family GTPases in cell polarisation and directional migration. *Curr. Opin. Cell Biol.* **15**, 590-597.
Ganz, A., Lambert, M., Saez, A., Silberzan, P., Buguin, A., Mege, R. M. and Ladoux, B. (2006). Traction forces exerted through N-cadherin contacts. *Biol. Cell.* **98**, 721-730.
Gavard, J., Lambert, M., Grosheva, I., Marthiens, V., Irinopoulou, T., Riou, J. F., Bershadsky, A. and Mège, R. M. (2004). Lamellipodium extension and cadherin adhesion: two cell responses to cadherin activation relying on distinct signalling pathways. *J. Cell Sci.* **117**, 257-270.
Giannone, G., Mège, R. M. and Thoumine, O. (2009). Multi-level molecular clutches in motile cell processes. *Trends Cell Biol.* **19**, 475-486.
Gomes, E. R., Jani, S. and Gundersen, G. G. (2005). Nuclear movement regulated by Cdc42, MRCK, myosin, and actin flow establishes MTOC polarization in migrating cells. *Cell* **121**, 451-463.
Gumbiner, B., Stevenson, B. and Grimaldi, A. (1988). The role of the cell adhesion molecule uvomorulin in the formation and maintenance of the epithelial junctional complex. *J. Cell Biol.* **107**, 1575-1587.
Hazan, R. B., Qiao, R., Keren, R., Badano, I. and Suyama, K. (2004). Cadherin switch in tumor progression. *Ann. N. Y. Acad. Sci.* **1014**, 155-163.
Huda, S., Soh, S., Pilans, D., Byrska-Bishop, M., Kim, J., Wilk, G., Borisy, G. G., Kandere-Grzybowska, K. and Grzybowski, B. A. (2012). Microtubule guidance tested through controlled cell geometry. *J. Cell Sci.* **125**, 5790-5799.
Ivanov, A. I., McCall, I. C., Parkos, C. A. and Nusrat, A. (2004). Role for actin filament turnover and a myosin II motor in cytoskeleton-driven disassembly of the epithelial apical junctional complex. *Mol. Biol. Cell* **15**, 2639-2651.
Ivanov, A. I., McCall, I. C., Babbin, B., Samarin, S. N., Nusrat, A. and Parkos, C. A. (2006). Microtubules regulate disassembly of epithelial apical junctions. *BMC Cell Biol.* **7**, 12.
Jaulin, F. and Kreitzer, G. (2010). KIF17 stabilizes microtubules and contributes to epithelial morphogenesis by acting at MT plus ends with EB1 and APC. *J. Cell Biol.* **190**, 443-460.
Jossin, Y. and Cooper, J. A. (2011). Reelin, Rap1 and N-cadherin orient the migration of multipolar neurons in the developing neocortex. *Nat. Neurosci.* **14**, 697-703.
Kadir, S., Astin, J. W., Tahtamouni, L., Martin, P. and Nobes, C. D. (2011). Microtubule remodelling is required for the front-rear polarity switch during contact inhibition of locomotion. *J. Cell Sci.* **124**, 2642-2653.
Kadowaki, M., Nakamura, S., Machon, O., Krauss, S., Radice, G. L. and Takeichi, M. (2007). N-cadherin mediates cortical organization in the mouse brain. *Dev. Biol.* **304**, 22-33.
Kaverina, I., Rottner, K. and Small, J. V. (1998). Targeting, capture, and stabilization of microtubules at early focal adhesions. *J. Cell Biol.* **142**, 181-190.
Kawauchi, T., Sekine, K., Shikanai, M., Chihama, K., Tomita, K., Kubo, K., Nakajima, K., Nabeshima, Y. and Hoshino, M. (2010). Rab GTPases-dependent endocytic pathways regulate neuronal migration and maturation through N-cadherin trafficking. *Neuron* **67**, 588-602.
Kee, S. H. and Steinert, P. M. (2001). Microtubule disruption in keratinocytes induces cell-cell adhesion through activation of endogenous E-cadherin. *Mol. Biol. Cell* **12**, 1983-1993.
Komarova, Y., De Groot, C. O., Grigoriev, I., Gouveia, S. M., Munteanu, E. L., Schober, J. M., Honnappa, S., Buey, R. M., Hoogenraad, C. C., Dogterom, M. et al. (2009). Mammalian end binding proteins control persistent microtubule growth. *J. Cell Biol.* **184**, 691-706.

Komarova, Y. A., Huang, F., Geyer, M., Daneshjou, N., Garcia, A., Idalino, L., Kreutz, B., Mehta, D. and Malik, A. B. (2012). VE-cadherin signaling induces EB3 phosphorylation to suppress microtubule growth and assemble adherens junctions. *Mol. Cell* **48**, 914-925.

Ladoux, B., Anon, E., Lambert, M., Rabodzey, A., Hersen, P., Buguin, A., Silberzan, P. and Mège, R. M. (2010). Strength dependence of cadherin-mediated adhesions. *Biophys. J.* **98**, 534-542.

Lambert, M., Padilla, F. and Mège, R. M. (2000). Immobilized dimers of N-cadherin-Fc chimera mimic cadherin-mediated cell contact formation: contribution of both outside-in and inside-out signals. *J. Cell Sci.* **113**, 2207-2219.

Lelièvre, E. C., Plestant, C., Boscher, C., Wolff, E., Mège, R. M. and Birbes, H. (2012). N-cadherin mediates neuronal cell survival through Bim down-regulation. *PLoS ONE* **7**, e33206.

Ligon, L. A. and Holzbaur, E. L. (2007). Microtubules tethered at epithelial cell junctions by dynein facilitate efficient junction assembly. *Traffic* **8**, 808-819.

Ligon, L. A., Karki, S., Tokito, M. and Holzbaur, E. L. (2001). Dynein binds to beta-catenin and may tether microtubules at adherens junctions. *Nat. Cell Biol.* **3**, 913-917.

Lorenowicz, M. J., Fernandez-Borja, M., van Stalborch, A. M., van Sterkenburg, M. A., Hiemstra, P. S. and Hordijk, P. L. (2007). Microtubule dynamics and Rac-1 signaling independently regulate barrier function in lung epithelial cells. *Am. J. Physiol.* **293**, L1321-L1331.

Mary, S., Charrasse, S., Meriane, M., Comunale, F., Travo, P., Blangy, A. and Gauthier-Rouvière, C. (2002). Biogenesis of N-cadherin-dependent cell-cell contacts in living fibroblasts is a microtubule-dependent kinesin-driven mechanism. *Mol. Biol. Cell* **13**, 285-301.

Mège, R. M., Matsuzaki, F., Gallin, W. J., Goldberg, J. I., Cunningham, B. A. and Edelman, G. M. (1988). Construction of epithelioid sheets by transfection of mouse sarcoma cells with cDNAs for chicken cell adhesion molecules. *Proc. Natl. Acad. Sci. USA* **85**, 7274-7278.

Mège, R. M., Gavard, J. and Lambert, M. (2006). Regulation of cell-cell junctions by the cytoskeleton. *Curr. Opin. Cell Biol.* **18**, 541-548.

Meijering, E., Dzyubachyk, O. and Smal, I. (2012). Methods for cell and particle tracking. *Methods Enzymol.* **504**, 183-200.

Meng, W., Mushika, Y., Ichii, T. and Takeichi, M. (2008). Anchorage of microtubule minus ends to adherens junctions regulates epithelial cell-cell contacts. *Cell* **135**, 948-959.

Myers, K. A., Applegate, K. T., Danuser, G., Fischer, R. S. and Waterman, C. M. (2011). Distinct ECM mechanosensing pathways regulate microtubule dynamics to control endothelial cell branching morphogenesis. *J. Cell Biol.* **192**, 321-334.

Nabi, I. R. (1999). The polarization of the motile cell. *J. Cell Sci.* **112**, 1803-1811.

Ouyang, M., Lu, S., Kim, T., Chen, C. E., Seong, J., Leckband, D. E., Wang, F., Reynolds, A. B., Schwartz, M. A. and Wang, Y. (2013). N-cadherin regulates spatially polarized signals through distinct p120ctn and β-catenin-dependent signalling pathways. *Nat. Commun.* **4**, 1589.

Palazzo, A. F., Eng, C. H., Schlaepfer, D. D., Marcantonio, E. E. and Gundersen, G. G. (2004). Localized stabilization of microtubules by integrin- and FAK-facilitated Rho signaling. *Science* **303**, 836-839.

Peris, L., Thery, M., Fauré, J., Saoudi, Y., Lafanechère, L., Chilton, J. K., Gordon-Weeks, P., Galjart, N., Bornens, M., Wordeman, L. et al. (2006). Tubulin tyrosination is a major factor affecting the recruitment of CAP-Gly proteins at microtubule plus ends. *J. Cell Biol.* **174**, 839-849.

Ponti, A., Machacek, M., Gupton, S. L., Waterman-Storer, C. M. and Danuser, G. (2004). Two distinct actin networks drive the protrusion of migrating cells. *Science* **305**, 1782-1786.

Prager-Khoutorsky, M., Lichtenstein, A., Krishnan, R., Rajendran, K., Mayo, A., Kam, Z., Geiger, B. and Bershadsky, A. D. (2011). Fibroblast polarization is a matrix-rigidity-dependent process controlled by focal adhesion mechanosensing. *Nat. Cell Biol.* **13**, 1457-1465.

Radice, G. L., Rayburn, H., Matsunami, H., Knudsen, K. A., Takeichi, M. and Hynes, R. O. (1997). Developmental defects in mouse embryos lacking N-cadherin. *Dev. Biol.* **181**, 64-78.

Ratheesh, A., Gomez, G. A., Priya, R., Verma, S., Kovacs, E. M., Jiang, K., Brown, N. H., Akhmanova, A., Stehbens, S. J. and Yap, A. S. (2012). Centralspindlin and α-catenin regulate Rho signalling at the epithelial zonula adherens. *Nat. Cell Biol.* **14**, 818-828.

Riedl, J., Crevenna, A. H., Kessenbrock, K., Yu, J. H., Neukirchen, D., Bista, M., Bradke, F., Jenne, D., Holak, T. A., Werb, Z. et al. (2008). Lifeact: a versatile marker to visualize F-actin. *Nat. Methods* **5**, 605-607.

Riehl, R., Johnson, K., Bradley, R., Grunwald, G. B., Cornel, E., Lilienbaum, A. and Holt, C. E. (1996). Cadherin function is required for axon outgrowth in retinal ganglion cells in vivo. *Neuron* **17**, 837-848.

Rodriguez, O. C., Schaefer, A. W., Mandato, C. A., Forscher, P., Bement, W. M. and Waterman-Storer, C. M. (2003). Conserved microtubule-actin interactions in cell movement and morphogenesis. *Nat. Cell Biol.* **5**, 599-609.

Shaw, R. M., Fay, A. J., Puthenveedu, M. A., von Zastrow, M., Jan, Y. N. and Jan, L. Y. (2007). Microtubule plus-end-tracking proteins target gap junctions directly from the cell interior to adherens junctions. *Cell* **128**, 547-560.

Shtutman, M., Chausovsky, A., Prager-Khoutorsky, M., Schiefermeier, N., Boguslavsky, S., Kam, Z., Fuchs, E., Geiger, B., Borisy, G. G. and Bershadsky, A. D. (2008). Signaling function of alpha-catenin in microtubule regulation. *Cell Cycle* **7**, 2377-2383.

Small, J. V. and Kaverina, I. (2003). Microtubules meet substrate adhesions to arrange cell polarity. *Curr. Opin. Cell Biol.* **15**, 40-47.

Stehbens, S. and Wittmann, T. (2012). Targeting and transport: how microtubules control focal adhesion dynamics. *J. Cell Biol.* **198**, 481-489.

Stehbens, S. J., Paterson, A. D., Crampton, M. S., Shewan, A. M., Ferguson, C., Akhmanova, A., Parton, R. G. and Yap, A. S. (2006). Dynamic microtubules regulate the local concentration of E-cadherin at cell-cell contacts. *J. Cell Sci.* **119**, 1801-1811.

Stehbens, S. J., Akhmanova, A. and Yap, A. S. (2009). Microtubules and cadherins: a neglected partnership. *Front. Biosci.* **14**, 3159-3167.

Stepanova, T., Slemmer, J., Hoogenraad, C. C., Lansbergen, G., Dortland, B., De Zeeuw, C. I., Grosveld, F., van Cappellen, G., Akhmanova, A. and Galjart, N. (2003). Visualization of microtubule growth in cultured neurons via the use of EB3-GFP (end-binding protein 3-green fluorescent protein). *J. Neurosci.* **23**, 2655-2664.

Straube, A. and Merdes, A. (2007). EB3 regulates microtubule dynamics at the cell cortex and is required for myoblast elongation and fusion. *Curr. Biol.* **17**, 1318-1325.

Taniguchi, H., Kawauchi, D., Nishida, K. and Murakami, F. (2006). Classic cadherins regulate tangential migration of precerebellar neurons in the caudal hindbrain. *Development* **133**, 1923-1931.

Teng, J., Rai, T., Tanaka, Y., Takei, Y., Nakata, T., Hirasawa, M., Kulkarni, A. B. and Hirokawa, N. (2005). The KIF3 motor transports N-cadherin and organizes the developing neuroepithelium. *Nat. Cell Biol.* **7**, 474-482.

Trichet, L., Le Digabel, J., Hawkins, R. J., Vedula, S. R., Gupta, M., Ribrault, C., Hersen, P., Voituriez, R. and Ladoux, B. (2012). Evidence of a large-scale mechanosensing mechanism for cellular adaptation to substrate stiffness. *Proc. Natl. Acad. Sci. USA* **109**, 6933-6938.

Vasquez, R. J., Howell, B., Yvon, A. M., Wadsworth, P. and Cassimeris, L. (1997). Nanomolar concentrations of nocodazole alter microtubule dynamic instability in vivo and in vitro. *Mol. Biol. Cell* **8**, 973-985.

Watanabe, T., Noritake, J., Kakeno, M., Matsui, T., Harada, T., Wang, S., Itoh, N., Sato, K., Matsuzawa, K., Iwamatsu, A. et al. (2009). Phosphorylation of CLASP2 by GSK-3beta regulates its interaction with IQGAP1, EB1 and microtubules. *J. Cell Sci.* **122**, 2969-2979.

Waterman-Storer, C. M., Salmon, W. C. and Salmon, E. D. (2000). Feedback interactions between cell-cell adherens junctions and cytoskeletal dynamics in newt lung epithelial cells. *Mol. Biol. Cell* **11**, 2471-2483.

Zamir, E., Katz, M., Posen, Y., Erez, N., Yamada, K. M., Katz, B. Z., Lin, S., Lin, D. C., Bershadsky, A., Kam, Z. et al. (2000). Dynamics and segregation of cell-matrix adhesions in cultured fibroblasts. *Nat. Cell Biol.* **2**, 191-196.

Zhang, T., Zaal, K. J., Sheridan, J., Mehta, A., Gundersen, G. G. and Ralston, E. (2009). Microtubule plus-end binding protein EB1 is necessary for muscle cell differentiation, elongation and fusion. *J. Cell Sci.* **122**, 1401-1409.

SUPPLENTAL FIGURE LEGENDS

Figure S1: Distribution of actin and MT networks in MDCK spread on Ecad-Fc.
Epithelial MDCK cells were spread for 2 hours on Ecad-Fc coated surfaces, fixed and immunostained for F-actin and tubulin. Scale bars: 10 μm.

Figure S2: Characterization of MT maturation in cells spread on Ncad-Fc and FN substrates.
Immunostaining for specific post-translationally modified forms of α-tubulin in cells plated on Ncad-Fc and FN. Tyrosinated tubulin (tyr) was the major form of tubulin found incorporated in MTs both on Ncad-Fc and Fn. More stable detyrosinated MTs (de-tyr; recognized by anti-Glu antibodies) were completely absent from cells plated on both Ncad-Fc and FN. Acetylated MTs (ace) were also absent from cells seeded on Ncad-Fc but detected in as small fragments in the center of cells seeded on FN. Scale bars: 10 μm.

Figure S3: Distribution of MT plus ends in cell monolayers and cells spread on Ncad-Fc substrates.
(A) C2C12 cell monolayers were either stained for β-catenin (red) and α-tubulin (green) on the left, or β-catenin (red) and EB1 (green) on the right. Cell-cell contacts are indicated with asterisks. **(B)** Cells expressing EB1-GFP were plated either on Ncad-Fc or FN for 2 hrs, then stained with anti-β-catenin (red) and anti-α-tubulin (green) antibodies. In cells spread on Ncad-Fc, MTs and comet-like EB1 accumulations decorating growing MT plus ends rarely populate the lamellipodium zone were are formed cadherin adhesions; the comets were frequently oriented tangential to the cell edge (top). In contrast, these comets at the tip of MTs were directed towards and reached the lamellipodium edge of cells spread on FN. Higher magnifications of boxed areas of cells spread on Ncad-Fc (b1) and FN (b2) are shown at the bottom. Scale bars: 10 μm.

Figure S4: Effect of the expression of the DN-Ncad mutant on MT penetration.
(A) Cells transfected with either WT Ncad (top) or DN Ncad (bottom) constructs plated on Ncad-Fc were immunostained for β-catenin and α-tubulin. Cadherin adhesion formation and actin treadmilling were not impaired in cells expressing low levels of DN Ncad, although their spreading was reduced (data not shown). **(B)** This moderate expression of DN Ncad did not

affect MT distribution either on Ncad-Fc or on FN. Scale bars 10 µm. Statistical analysis: One way ANOVA, ** p value <0.001; *** p value: <0.0001.

Figure S5: Effect of Cytochalasin D and blebbistatin treatments on F-actin and MT organization.

Cells spread on Ncad-Fc were treated with DMSO, cytochalasin D 100nM or blebbistatin 20 µM during 20 min, then fixed and stained for β-catenin, F-actin and MTs. Cytochalasin D treatment induced a disorganization of actin cytoskeleton in parallel of an extension of the MT networks towards the cell edges. The inhibition of myosin II activity by blebbistatin triggered similar although less drastic effects on actin and MT networks. The dashed lines on the right panels indicate the edge of the cells. Scale bar 10 µm.

Supplementary movie S1. **EB3-mCherry comet movements in C2 cells plated on fibronectin**.

One day post-transfection cells were dissociated in trypsin-free conditions and acquisitions were performed 2 hrs after plating on FN with a spinning disk. EB3 comets are numerous and generally travel towards the cell periphery. 20 frames/s, total duration 5 min.

Supplementary movie S2. **EB3-mCherry comet movements in C2 cells plated on Ncad-Fc.**

One day post-transfection cells were dissociated in trypsin-free conditions and acquisitions were performed 2 hrs after plating on Ncad-Fc with a spinning disk. EB3 comets can loop before entering the adhesion area and move towards the cell periphery, but few of them can reach the cell border. 20 frames/s, total duration 5 min.

Supplementary movie S3. **EB3-GFP movements in cells plated on Ncad-Fc, before and after cytochalasin D treatment.**

Cells were co-transfected with N-cadherin-DsRed and EB3-GFP one day before live cell imaging. Image acquisitions were performed before treatment, and resumed after 20 minutes of incubation with cytochalasin D 100 nM. 20 frames/s, total duration 1 min before treatment and 1 min after treatment.

Supplementary movie S4. **EB3-GFP movements in cells plated on Ncad-Fc substrate, before and after blebbistatin treatment.**

The experimental conditions are the same as for supplementary movie S3, blebbistatin 20 µM replacing cytochalasin D treatment.

Supplementary movie S5. Actin dynamics in cells plated on Ncad-Fc substrate.

Cells were transfected with Lifeact-GFP one day before live cell imaging and plated on Ncad-Fc substrate. Interval acquisition 1 s, total duration 5 min.

Supplementary movie S6. Actin dynamics in cells plated on FN substrate.

Cells were transfected with Lifeact-GFP one day before live cell imaging and plated on FN substrate. Interval acquisition 1 s, total duration 5 min.

Figure S1

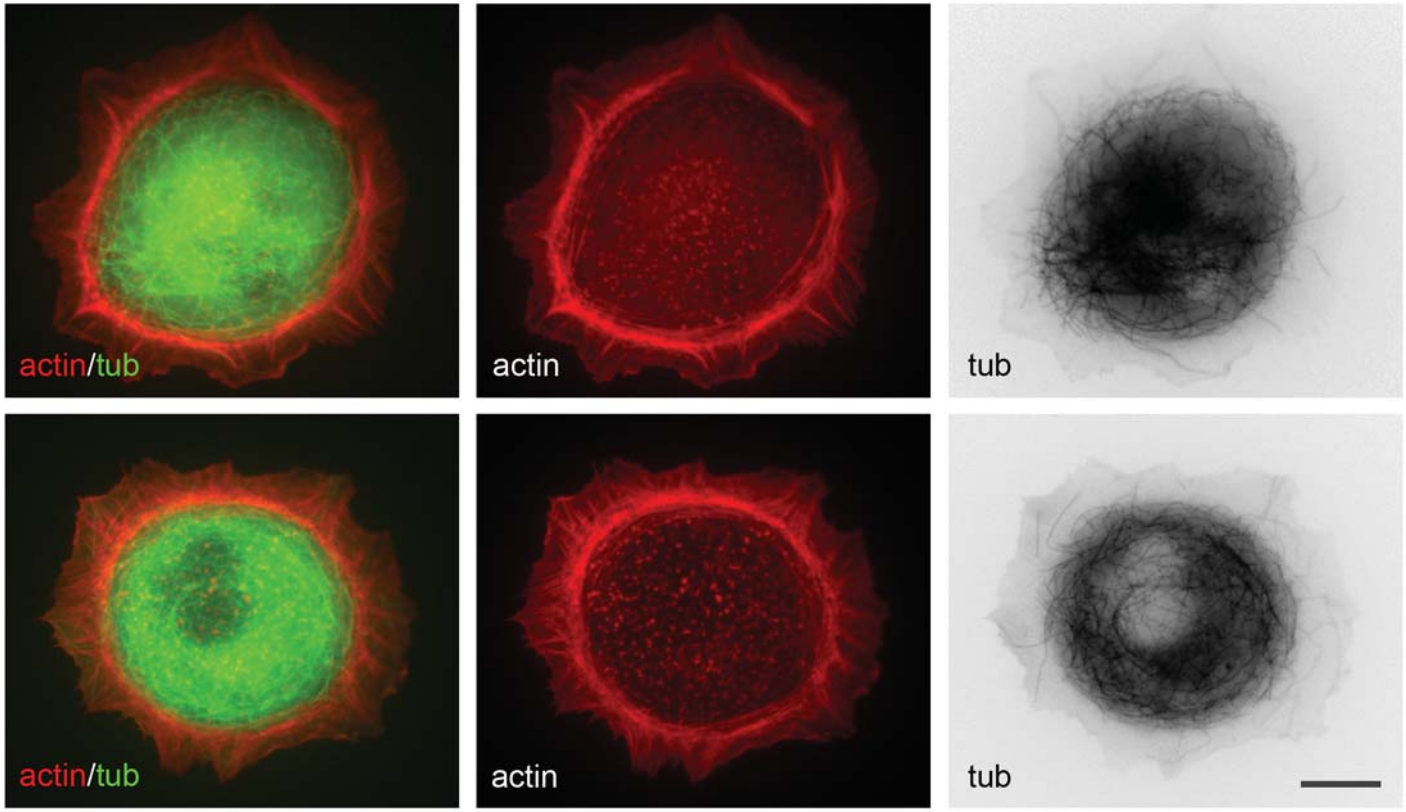

Figure S2

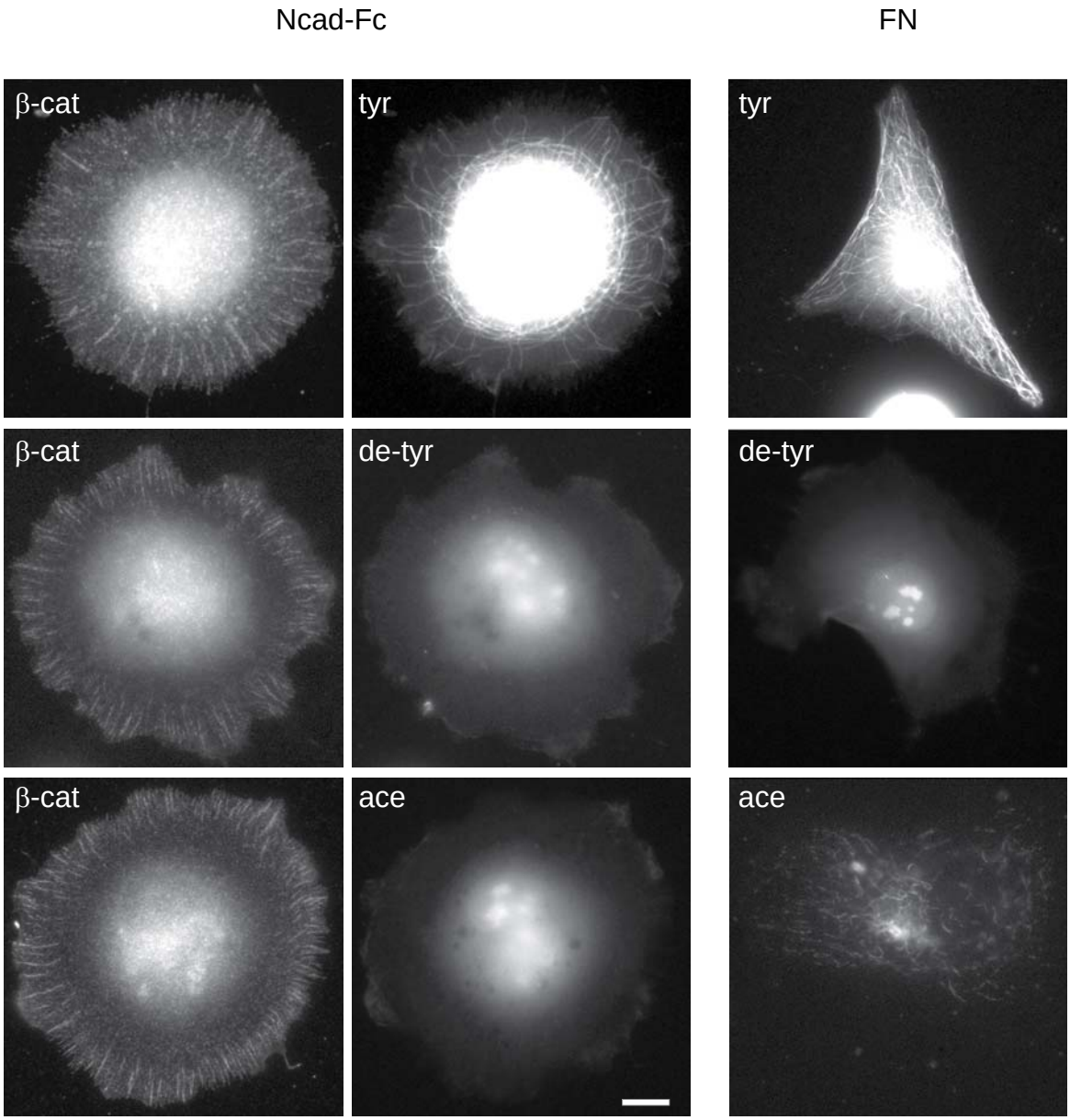

Figure S3

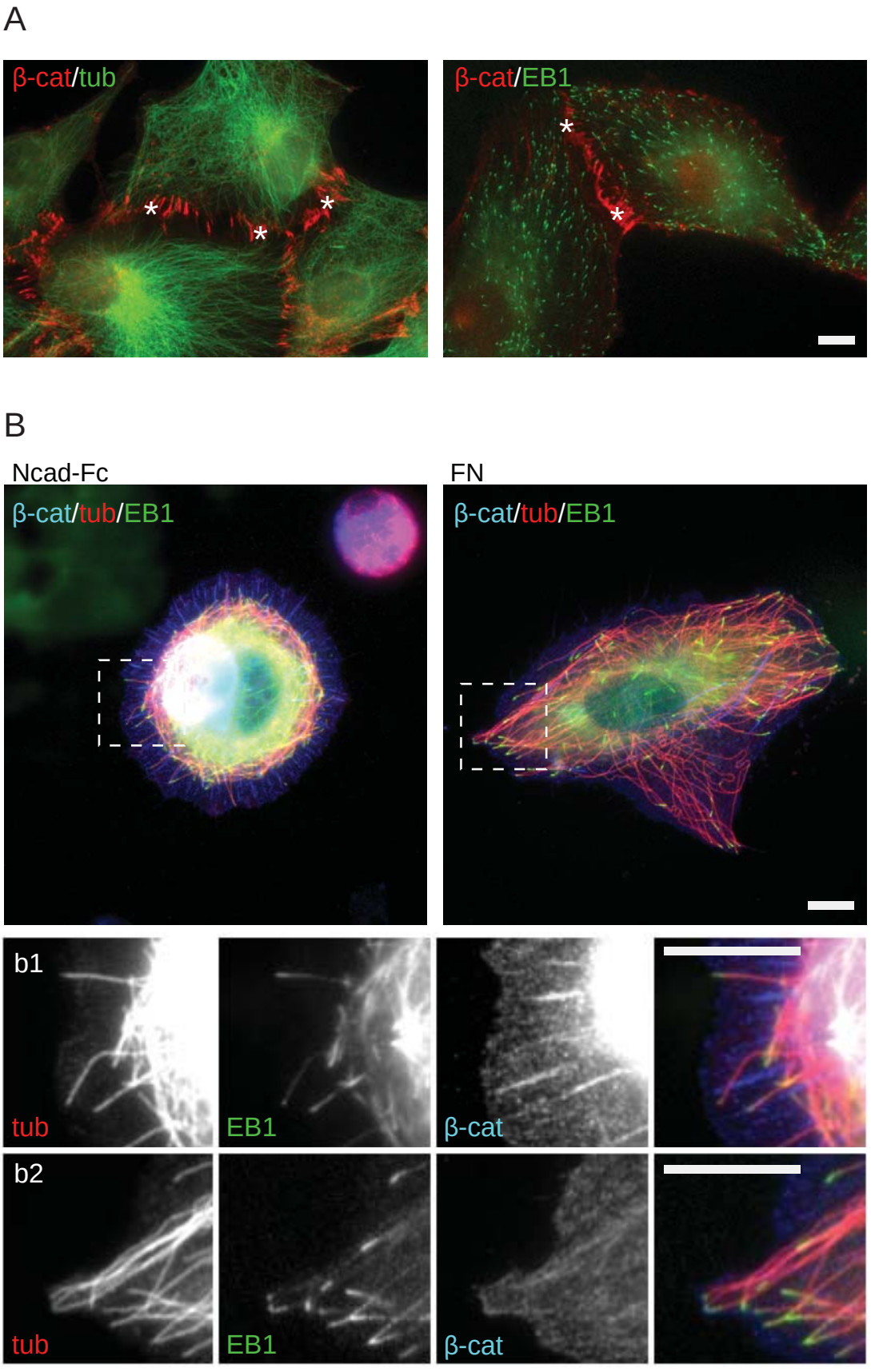
A
β-cat/tub
β-cat/EB1
B
Ncad-Fc
FN
β-cat/tub/EB1
β-cat/tub/EB1
b1
tub
EB1
β-cat
b2
tub
EB1
β-cat

Figure S4

A

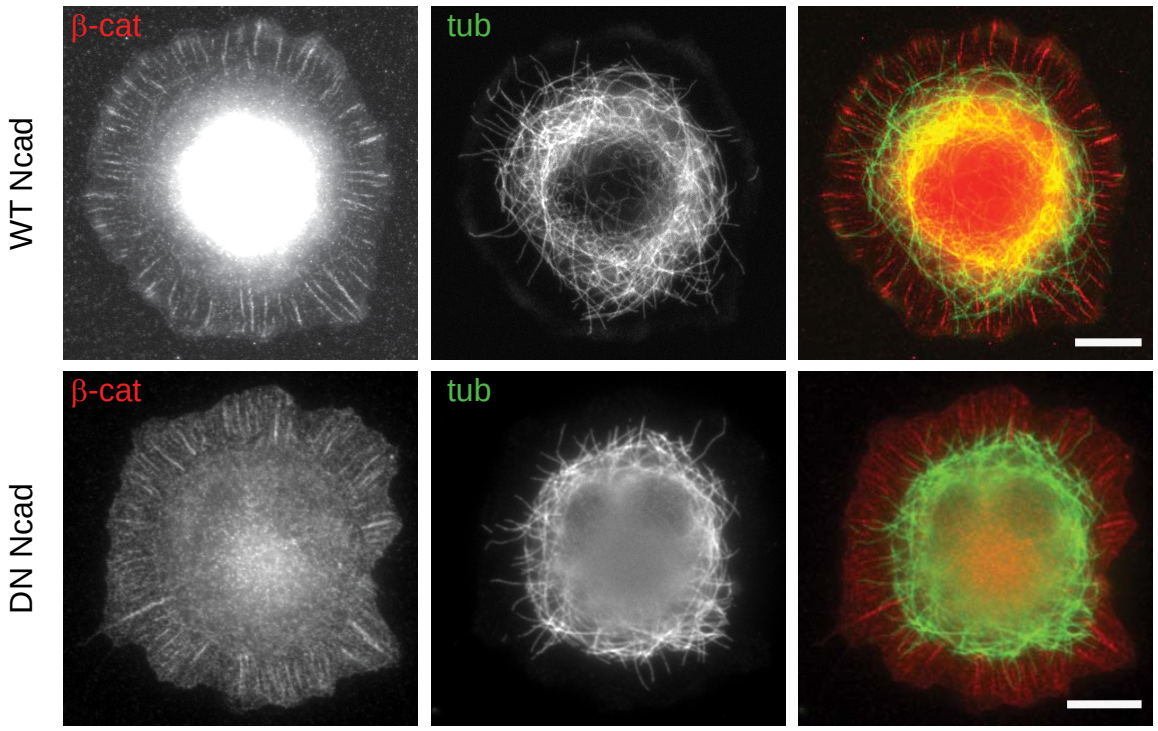
β-cat
tub
WT Ncad
β-cat
tub
DN Ncad

B

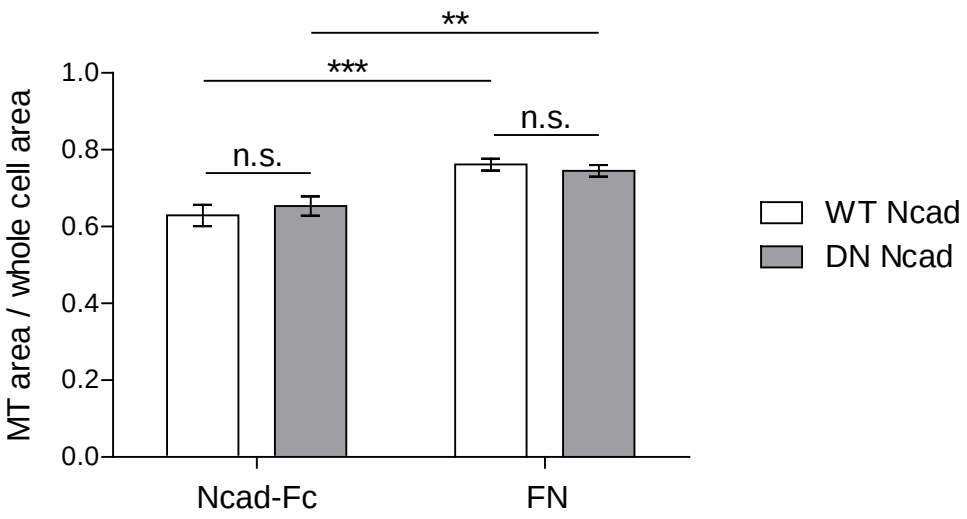
**
***
n.s.
n.s.
1.0
0.8
0.6
0.4
0.2
0.0
MT area / whole cell area
Ncad-Fc
FN
WT Ncad
DN Ncad

Figure S5

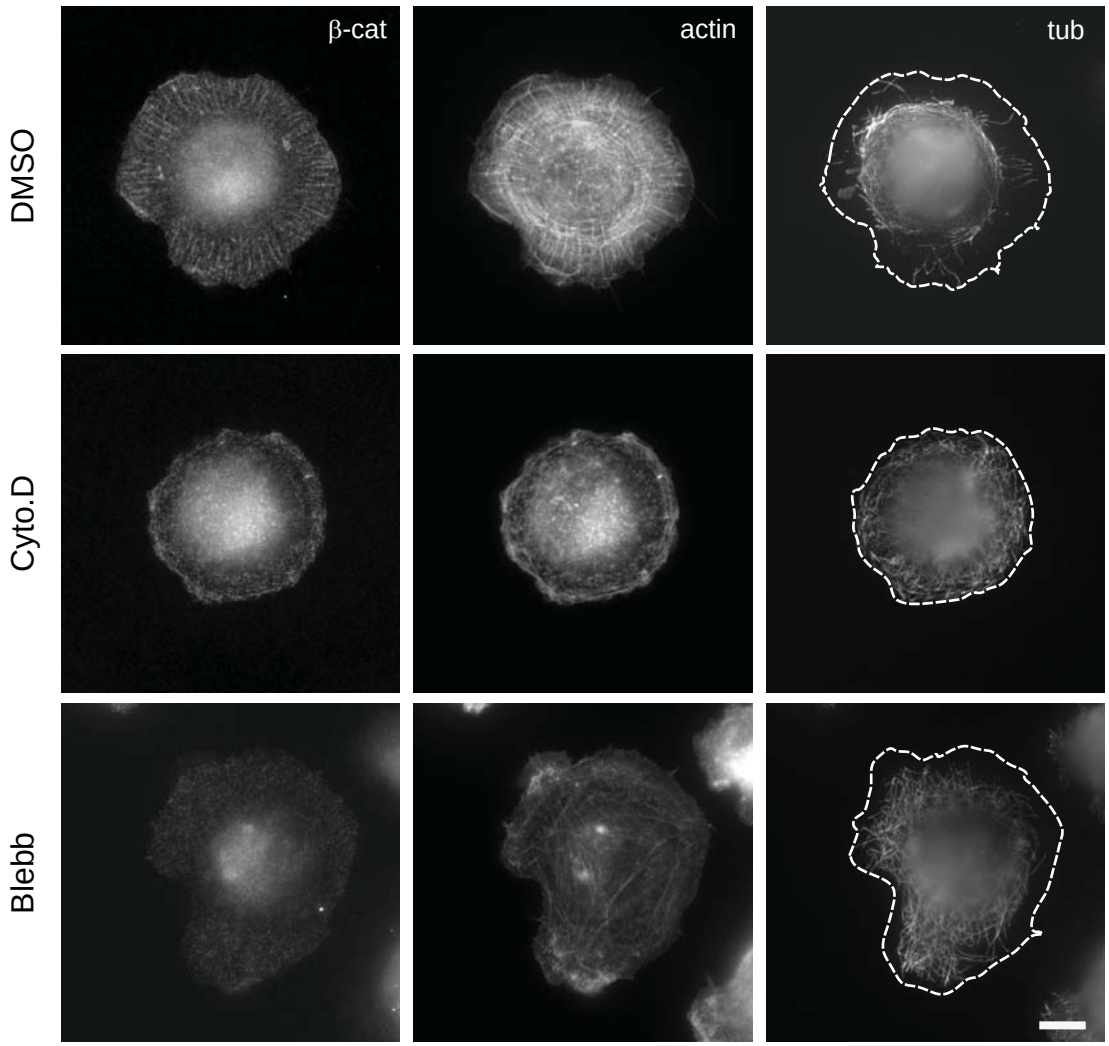

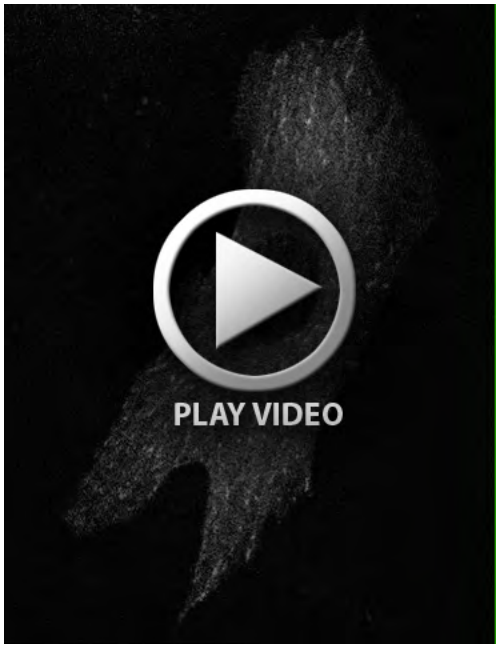

Movie 1.

Movie 2.

Movie 3.

Movie 4.

Movie 5.

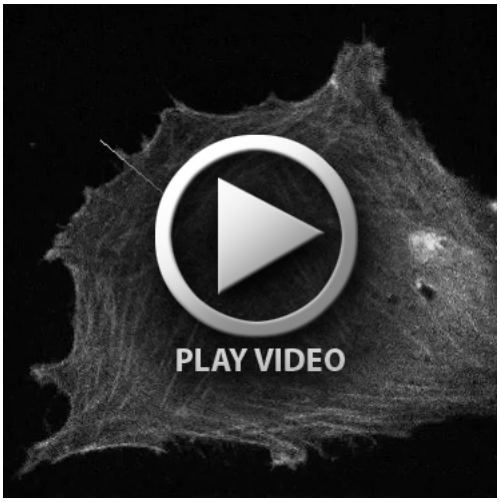

Movie 6.